Graz University of Technology

Development of an analytical code for soil nailing systems - considering tension and shear resistance of the nails

Masterarbeit zum Erwerb des

akademischen Titels Diplomingenieur der

Studienrichtung Bauingenieurwesen

Atieh Mirzaei

Verfasst am Institut für

Bodenmechanik und Grundbau

der Technischen Universität Graz

Betreuer der Masterarbeit:

Univ.-Prof. Dipl.-Ing. Dr.techn. Roman Marte

Dipl.-Ing. Dr.techn. Gregor Supp

Begutachter der Masterarbeit:

Univ.-Prof. Dipl.-Ing. Dr.techn. Roman Marte

Graz, September 2015

Eidesstattliche Erklärung

Ich erkläre an Eides statt, dass ich die vorliegende Arbeit selbstständig verfasst, andere als die angegebenen Quellen/Hilfsmittel nicht benutzt und die den benutzten Quellen wörtlich und inhaltlich entnommenen Stellen als solche kenntlich gemacht habe.

Statutory Declaration

I declare that I have authored this thesis independently, that I have not used other than the declared sources / resources and that I have explicitly marked all material which has been quoted either literally or by content from the used sources.

Graz, am …… ……

(Atieh Mirzaei)

Acknowledgement

I would like to express my special gratitude and thanks to my advisor Professor Dr. Roman Marte, you have been a tremendous mentor for me. I would like to thank you for the useful comments, remarks and engagement through the learning process of this master thesis.

I would also gratefully and sincerely thank Dr. Gregor Supp for his guidance, understanding, patience, and most importantly, his friendship during my graduate studies.

Thanks to my family and friends who offered invaluable support and humor over the years. My thanks and appreciations also go to my parents. Words cannot express how grateful I am for all of the sacrifices that you've made on my behalf. Your prayer for me was what sustained me thus far. At the end I would like to express appreciation to my beloved husband Mohammad who spent sleepless nights with and was always my support in the moments when there was no one to answer my queries.

Dedication

This thesis work is dedicated to my parents who have always loved me unconditionally and whose good examples have taught me to work hard for the things that I aspire to achieve.

This work is also dedicated to my husband, Mohammad, who has been a constant source of support and encouragement during the challenges of graduate and life. I am truly thankful for having you in my life.

Abstract

Soil nailing has been widely used to stabilize slopes and excavations in the last few decades. The soil nail as a passive inclusion particularly improves the stability of geotechnical engineering structures by mobilizing the axial frictional resistance in the passive zone. A method of evaluation of the in-soil deformation of the nail is discussed based on the simplified hypotheses regarding frictional properties between soil and nail and tensile force vs. strain relationship of nail material. By solving the derived differential equation based on the assumptions, distribution of relative displacement, shear stresses and tensile forces acting any part of the nail can be calculated. Moreover, the tensile and shear forces mobilized in the nail at the intersection with failure surface depending on relative displacements between soil and nail regarding to circular slope rotation can be also obtained.

The concept and principals involved in different methods of slope stability analysis of slopes have been discussed. Theoretical studies have shown that a common formulation of the equilibrium equations can be used for all of the methods. The factor of safety has been derived with respect to either moment equilibrium or force equilibrium or both of these equations. The mathematical equations and the methodology for assessing the factor of safety of reinforced soil slope of any specified (chosen) slip circle by Bishop and Spencer methods have been given. The forces which act within a soil mass have been discussed. The interslice normal and shear forces which are being also considered in Spencer method have been described and mathematical equations given to calculate them for the analysis. The specified function $f\ (x)$ (constant function) and applied function ratio indicated by 'λ' has been explained.

An analytical code has been developed by MATLAB software to simulate a specified soil nail reinforced slope. This Program uses an iterative method to calculate the mobilized displacements along and normal to the nail at the failure surface by considering some assumptions regarding the variation of slope rotation angles. Consequently resisting forces (tensile and shear forces) developed in the nail are calculated. To analyzing the slope stability reinforced with nails additionally, the codes are developed using both Bishop and Spencer methods. Since calculating Spencer factor of safety for a reinforced slope needs assumptions which make this method extremely complex, further research

works will be necessary. Therefore the factor of safety results from the Bishop method which includes interslice normal forces and satisfies only moment equilibrium.

Nomenclature

D = Diameter of the nail

EI = Bending stiffness of the nail

c' = Effective cohesion

ϕ' = Effective angle of internal friction

k_s = Modulus of lateral soil reaction

s = Shear strength

σ_n = Normal stress

$\tau(x)$ = Shear stress

S = Tensile stiffness of the nail

W = The total weight of a slice

P = The total normal force on the slice base

S_m = The shear force mobilized on the base of each slice

E = The horizontal interslice normal forces

X = The vertical interslice shear forces

R = The radius for a circular slip surface

A = The resultant external water forces

θ = The angle between the tangent to the center of the base of each slice and the horizontal

α = The angle of nail with horizontal

F = The factor of safety

T = Nail tensile force for the reinforcement emerging out from the slice base

F_s = Nail shear force mobilized at the intersection with failure surface

tp = Peak shear stress at the interface of soil and nail

up = Soil-nail displacement causing peak shear stress

Table of Contents

1 Introduction and Motivation

Soil nailing has been widely used to stabilize slopes and excavations in the last few decades. The soil nail as a passive composition principally improves the stability of geotechnical engineering structures by mobilizing the axial frictional resistance in the passive zone. (Hong et al. 2012). These days, a large number of mathematical approaches have been developed to simulate the fundamental interaction behavior between soil and soil inclusions (Abramento and Whittle 1995; Madhav et al. 1998; Gurung and Iwao 1999; Wang and Richwien 2002; Zhou and Yin 2008). These relationships include different parameters, such as the mobilized soil thickness at the interface, the soil shear modulus, the nail dimensions and elastic modulus of the nail. The design methods that have been mostly used are Davis (Mitchell 1987), German (Stocker and Riedinger 1990), and French methods (Schlosser et al. 1992), on which the limit equilibrium approaches are based (Juran and Elias 1987). Newly, a kinematical limit equilibrium design method has been introduced by Juran (Juran et al. 1990) and Byrne (Byrne 1992). This method provides estimated values of maximum tensile and shear forces mobilized in each reinforcement. In Juran's method, the normal stress distribution along the failure surface is evaluated by using Kotter's equation (Leshchinsky 1991). Therefore, the method has the advantage that a force developed in each nail can be obtained from the horizontal force equilibrium of the slice including a nail (Kim et al.1997). The objective of the research reported in this thesis was to study the in-soil deformation behavior of nail by taking the frictional properties and stiffness of each material into account. Based on some simplified assumptions an analytical model is proposed to describe the evolution of resisting forces along the nail regarding to relative displacement between soil and nail in the process of the failure of a slope. The slope stability analysis is done by Spencer and Bishop Methods. Compared with other methods Spencer takes both the interslice normal and shear forces and also provide moment equilibrium and force equilibrium into account giving both moment and force factor of safety. The Bishop method includes interslice normal forces and ignores the interslice shear forces and satisfies only moment equilibrium. This thesis presents the Spencer and Bishop methods in detail, and the advantage and limitations of different methods have also been discussed. An analytical code has been developed to make it possible to handle the

complexity of formulations proposed to describe the interaction mechanism between a soil nail and soil in the failure process. The codes are developed using both Bishop and Spencer methods. Since calculating Spencer factor of safety for a reinforced slope needs assumptions which make this method extremely complex, further research works will be necessary. Therefore the factor of safety results from the Bishop method.

2 Literature Review

2.1 The soil nailing technique

Soil nailing is a creation technique for reinforcing existing ground conditions. In general soil is a poor structural material because it is weak in tension. In contrast, steel is strong in tension. The basic concept of soil nailing is the support of soil by the installation of closely spaced, passive, steel bars, called ‘nails’, into a slope, to increase the overall shear force of the soil and hence, restrain displacement. The term ‘passive’ is applied. ‘Passive’ means that the nails are not pre-tensioned when installed and are forced to develop tension as the ground deforms laterally. Soil nails are used to stabilize either existing slopes or future slopes/cuts created by excavation activities at a site (Zhou and Yin 2008).

2.2 Behavior of a soil nailed system

A soil nailed system is recognized as a geotechnical structure, stabilized by soil nailing techniques, principally through the development of tensile force in the soil due to the nails. It can be a soil nailed slope, a soil nailed retaining wall, or a soil nailed excavation. The tensile forces are mobilized in the soil nails primarily through the frictional interaction between the soil nails and the ground, and the reactions provided by soil-nail heads/facing (Zhou and Yin 2008).

Two-zone model of a soil nailed system

Schlosser (1982) suggested a two-zone model to access the internal stability of a soil-nailed system. This model has been used in limit equilibrium analysis in soil nailing design, as shown in figure 2.1. The model divides the soil nailed system into two zones by potential failure surface, namely the active zone and the passive zone (or resistance zone). The active zone is the area in front of the potential failure surface, where it has a tendency to separate from the soil-nailed system and pull out the reinforcements. The passive zone is the region behind the potential failure surface, where the area remains more or less stable and prevents the sliding of the system. The soil nails act to tie (or

fasten) the active zone to the passive zone (Juran 1985, Jewell and Pedley 1990 and 1992, Bridle and Davies 1997).

As shown in figure 2.1, during the slope failure, the soil nail is not only faced with tensile forces but also shear forces and bending moments. These loads originate as reactions to the slope movement before and during the slope failure. To date, the common belief is that soil nails work predominantly in tension, but stresses are also mobilized due to shear and bending at the intersection of the slip surface with the soil nails (Juran 1985, Jewell and Pedley 1990 and 1992, Bridle and Davies 1997).

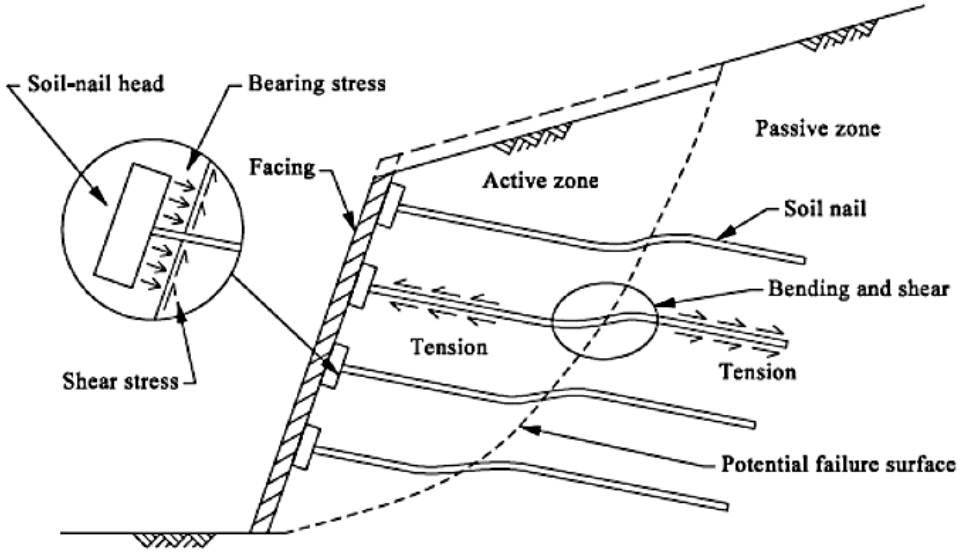

Figure 2.1. Two-zone model of a soil nailed system (after GEO 2008)

It should be noted that the two-zone model is only a simplification of the soil-nailed system for limit equilibrium analysis where the system deformation is not accounted for. In reality, instead of a slip surface, an irregular shearing failure zone is generally observed, as shown in figure 2.2. The interaction between the soil nail and surrounding soil is complex, and the forces developed in the soil nails are affected by many factors, Such as the nail features (i.e., tensile strength, shear strength and stiffness), the inclination of the soil nails, the soil characteristics (i.e., shear strength, saturation condition and gravel size), the friction between the soil nails and the soil, the size of soil-nail heads and the nature of the slope facing (Zhou 2008).

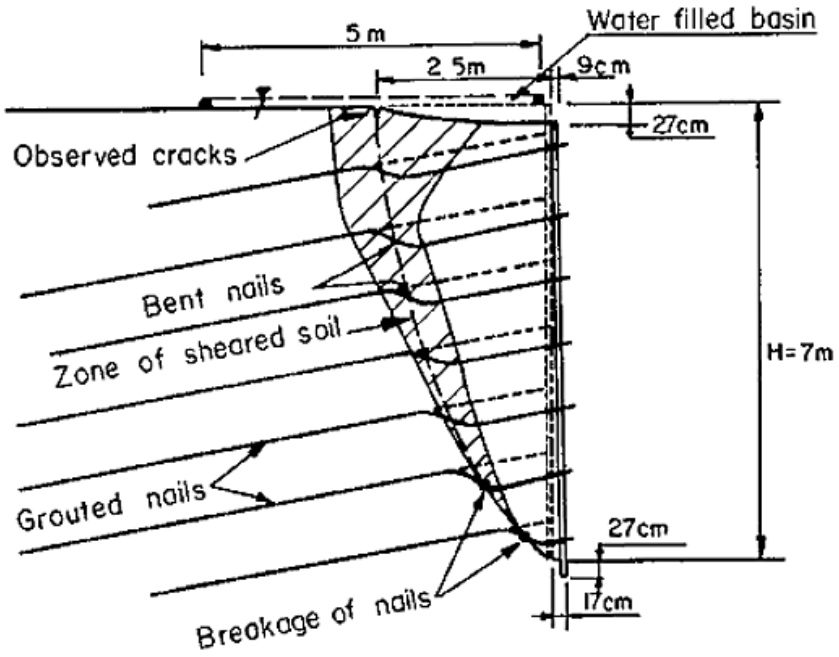

Figure 2.2. Post-failure observation of the first large-scale experimental soil nailed wall (Zhou 2008).

Tensile force distribution in the soil nails

The small displacements in a soil nailed system result in forces being mobilized in the soil nails. The major forces are axial tension, with bending moments and shear forces being of secondary importance. The tensile forces in the soil nail differ from the passive zone to the nail head: beginning as zero at the end of the nail, increasing to a maximum value in the intermediate length, and reducing to a value at the nail head. A schematic distribution of tensile forces in the soil nails are shown in figure 2.3. The locus of maximum tensile forces of soil nails and the potential failure surface of a slope are also shown in figure 2.3 (Zhou 2008).

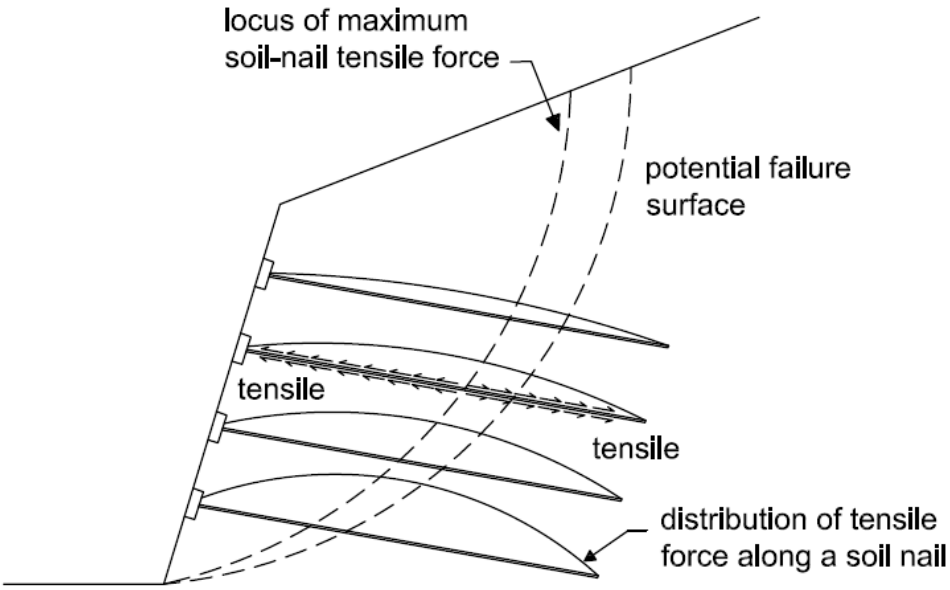

Figure 2.3. Schematic distribution of tensile forces along soil nails (after GEO 2008)

Gassler (1987) and Plumelle et al. (1990) reported that large bending moments take place in the reinforcement in place of the structure reaches collapse, at which point the observed displacements are large and the structure cannot be serviceable. Observed shear forces compared with the mobilized axial forces have been shown to be limited. In contrast to a consensus of concerning the mobilization and consideration of axial forces there is more discussion on the necessary consideration of shear forces for the design. There are some different suggestions regarding the stability calculations. The German code of practice for soil nailing, Institut fur Bautechnik (1986), Shen et al. (1981) (Davis method), Stocker and Reidinger (1990) and Kakurai and Hori (1990) take into account reinforcement axial force only. While the French design method suggested by Schlosser (1983) studies both shear and axial force in stability calculations, as do design methods proposed by Juran et al. (1990) and Bridle (1989). In other methods it is assumed that there is just one specific failure surface passing through the nailed structure; reinforcement crossing this surface is subjected to bearing stresses as a result of relative displacement of the soil on either side (figure 2.4). The amount of the shear force at the failure surface is a function of the lateral stress distribution on the reinforcement and is a maximum at this point. It is also considered in the above analyses that the interaction between the reinforcement and soil can be characterized by elastic parameters.

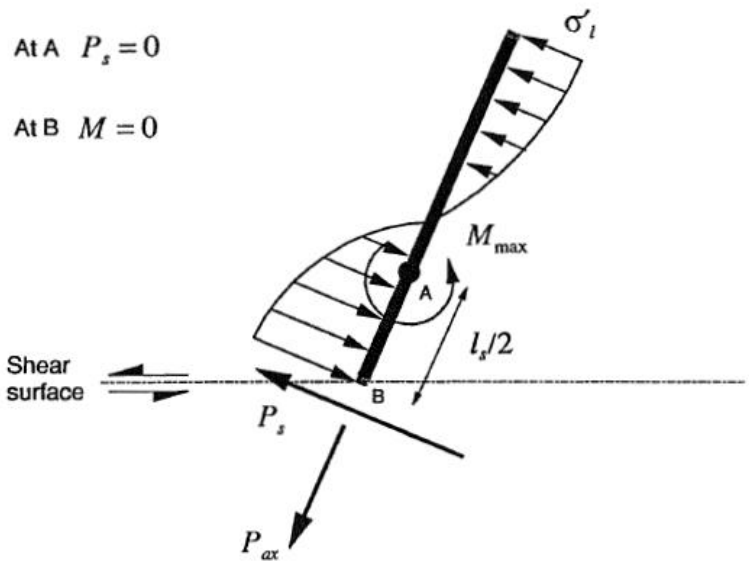

Figure 2.4. Bearing stresses acting on reinforcement on one side of a slip surface (Pedley 1990).

Delmas (1987) proved that including the reinforcement shear force in the calculation, led to a maximum increase in factor of safety of about 10%. Although the effect of shear force decreased rapidly as the density of reinforcement increased to typical quantities. (On the other hand investigating new nailing systems with larger diameters, other materials and etc.).

According to presented data, there is no doubt about the presence of both axial and shear force in soil nails. However there is still a great deal of uncertainty about the magnitude of the shear force and its effect on the stability of nailed structures; it is for this reason that many designers conservatively prefer to ignore the influence of reinforcement shear force (Pedley 1990).

2.3 Direct shear test

The shear strength parameters determination is critical since they are involved in the slope stability evaluation, the estimation of the risk of progressive failure and the evaluation of the engineering properties of soil deposits in stability problems (Bishop 1971). The ring shear apparatus and the direct shear Box permit to reach these parameters. Other devices (cone penetrometer, laboratory vane, plane strain and independent stress control ‘triaxial’, cellstriaxial apparatus) are also used (Bromhead

1992). At failure if stable yielding persists, the stress-strain curve is flat (Morgenstern and Tchalenko 1967). But for dilatant soils and soils with clay content greater than 30%, unstable yielding occurs requiring a negative stress increasing for a positive strain increment. Finally, stable yielding will be re-established at the residual strength where a dominant displacement discontinuity forms that can provide all further imposed deformation. These features are shown in figure 2.5.

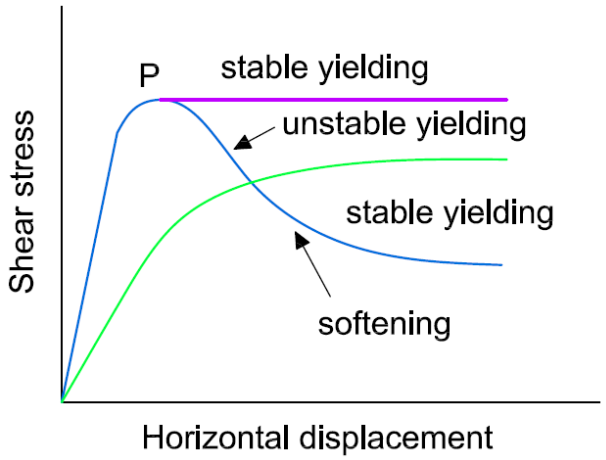

Figure 2.5. Typical stress-strain curve showing the stable and unstable yielding (Osano 2009).

Figure 2.5 describes peak and residual shear strength parameters. If shearing is continued after the peak point to the maximum displacement of the apparatus (for the ring shear), a curve of the type shown in figure 2.5 for the softening material is obtained (Manual of Soil Laboratory Testing 1994). At first, the shear strength decreases rapidly from the peak point, but finally reaches a steady state (ultimate) value, which describes the displacement increases.

The shear test is the oldest, the simplest and the most respective effective stresses for sufficient slow test procedure to present excess pore water pressure procedure for measuring the shear strength of soils in terms of total stresses. It is also the easiest to understand, but it has some shortcomings (Manual of Soil Laboratory Testing 1994). A diagram of the apparatus and the shearing action is shown in figure 2.6.

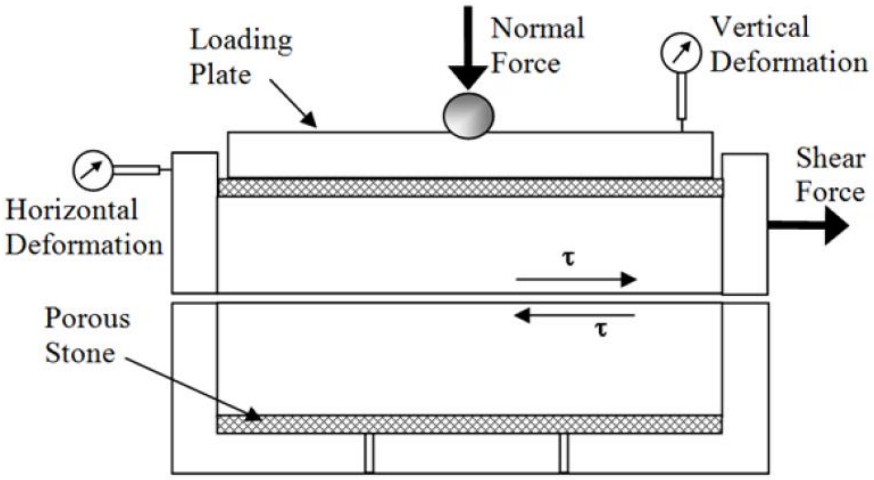

Figure 2.6. The shear box (http://www.iitgn.ac.in/research/stl/directshear.php).

The primary feature of the apparatus is a quadratic box, divided horizontally into two halves and containing a quadratic prism of soil. While a constant vertical compressive force is applied to the prism, the upper half of the box is subjected to an increasing horizontal force, therefore causing the prism to swear along the dividing plane of the box. Some identical specimens are tested using different vertical stresses so that a diagram of shearing resistance against vertical stress can be plotted. The vertical movement of the top surface of the specimen (volume changes) is also measured and enables changes in voids ratio and density during shear to be evaluated (Osano 2009).

2.4 Modeling of nail behavior

2.4.1 Mathematical Model of a Soil Nail Subjected to Pullout Force

To evaluate the pullout response of a soil nail in a soil nailing system a mathematical model was developed, which study the behavior of a soil nail section below the potential sliding surface. The soil nail is idealized as an isotropic, elastic inclusion. The effect of the pull out in the axial direction of a soil nail leads to the shear stress of the soil-nail interface, which is distributed uniformly in the diametrical direction. The radial deformation of the soil nail induced by axial pullout force is ignored. The pullout response of a soil nail element in a soil mass is shown in figure 2.7. A soil nail is subjected to external load (Gurung 2001; Misra et al. 2004; Misra and Chen 2004), force equilibrium is satisfied along the axial direction of the soil nail element as follows:

$$[T(x) + dT(x)] - T(x) - \tau(x)\pi D[du(x) + dx] = 0$$

(1)

where $T(x)$ and $T(x) + dT(x) =$ pullout forces at the two ends of the soil nail element (Figure 2.7); dx and $du(x) =$ length of nail element and the related length change caused by pullout force, respectively; and $\tau(x) =$ relevant pullout shear stress of the nail-soil interface. The preceding equation can be simplified as

$$\frac{dT(x)}{dx} - \tau(x)\pi D\left[\frac{du(x)}{dx} + 1\right] = 0$$

(2)

The strain of the nail element can be written in terms of the axial pullout force and is given as

$$\varepsilon(x) = \frac{T(x)}{EA} = \frac{du(x)}{dx}$$

(3)

Combining Eqs. (2) and (3) yields

$$EA\frac{du^2(x)}{dx^2} - \tau(x)\pi D[1 + \varepsilon(x)] = 0$$

(4)

Because the pullout strain $\varepsilon(x)$ is generally very small, Eq. (4) is approximated as

$$EA\frac{du^2(x)}{dx^2} - \tau(x)\pi D = 0$$

(5)

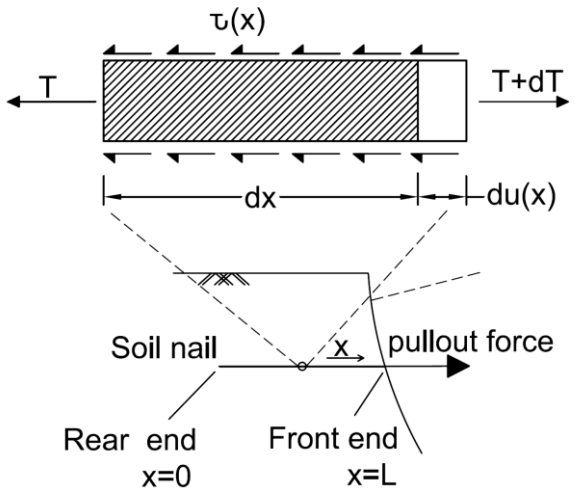

Figure 2.7. A schematic view of a soil nail element subjected to a pull out force in soil mass (modified from Mitachi et al. 1992).

A simple ideal load transfer model describing the relation between the shear stress $\tau(x)$ and pullout displacement $u(x)$ of the nail-soil interface at a distance of x from the nail tip is utilized (Guo 2001; Misra and Chen 2004), as shown in figure 2.8. The defined stiffness factor k may be taken from direct shear tests.

$$\tau = ku \qquad (u \leq u_p) \tag{6-1}$$

$$\tau = \tau_p \qquad (u > u_p) \tag{6-2}$$

$$k = \frac{\tau_p}{u_p} \tag{6-3}$$

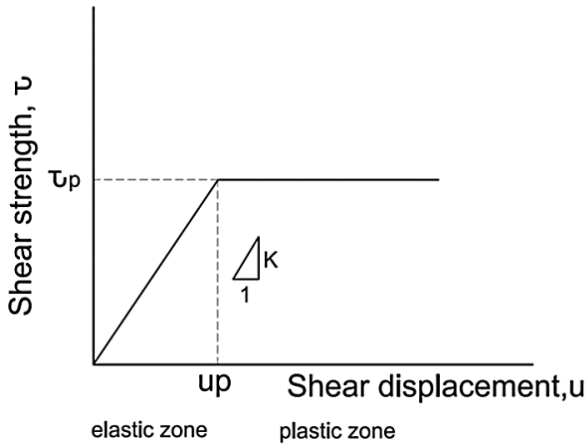

Figure 2.8. Load transfer model at the soil-nail interface during pullout of a nail (Hong et al. 2012).

In this model the shear stress of the nail-soil interface changes linearly with shear displacement in the elastic phase, but after the ultimate shear stress of the interface is approached, the shear stress becomes constant (Hong et al. 2012).

2.4.2 Tensile force

Soil nails as the passive inclusions require a soil displacement which leads to mobilize the resisting forces in the nails. Consequently, it is important to measure the frictional properties between soil and nails. The solution for tensile stresses developed in nails was

derived from the following assumption that has been proposed by Mitachi et al. (1992) in calculating the soil behavior of geo-grids.

The figure 2.8 shows the assumed frictional property at the interface. Combining equations of force equilibrium in the soil-nail system Eq. (5) with the frictional behavior Eqs. (6-1) and (6-2), the following differential equations are obtained.

$$\frac{d^2u}{dx^2} = \frac{D\pi k}{S}u \qquad (u \le u_p) \tag{7-1}$$

$$\frac{d^2u}{dx^2} = \frac{D\pi \tau_p}{S} \qquad (u > u_p) \tag{7-2}$$

Where $S =$ tensile stiffness of the nail $(= EA)$, $u =$ displacement between soil and nail in the direction of the nail length axis, $D =$ diameter of the nail, and $u_p =$ displacement mobilizing peak shear stress at the interface of soil and nail (Kim et al. 1997).

Distribution of relative displacement, frictional stress and tensile force developed in the nail

By solving Eq. (7) with boundary conditions, the distribution of relative displacement, frictional stress and tensile force developed in the nail are determined. According to the magnitude of the mobilized displacement, two different cases should be separately considered. All parameters which are used in the following equations are shown in figure 2.9.

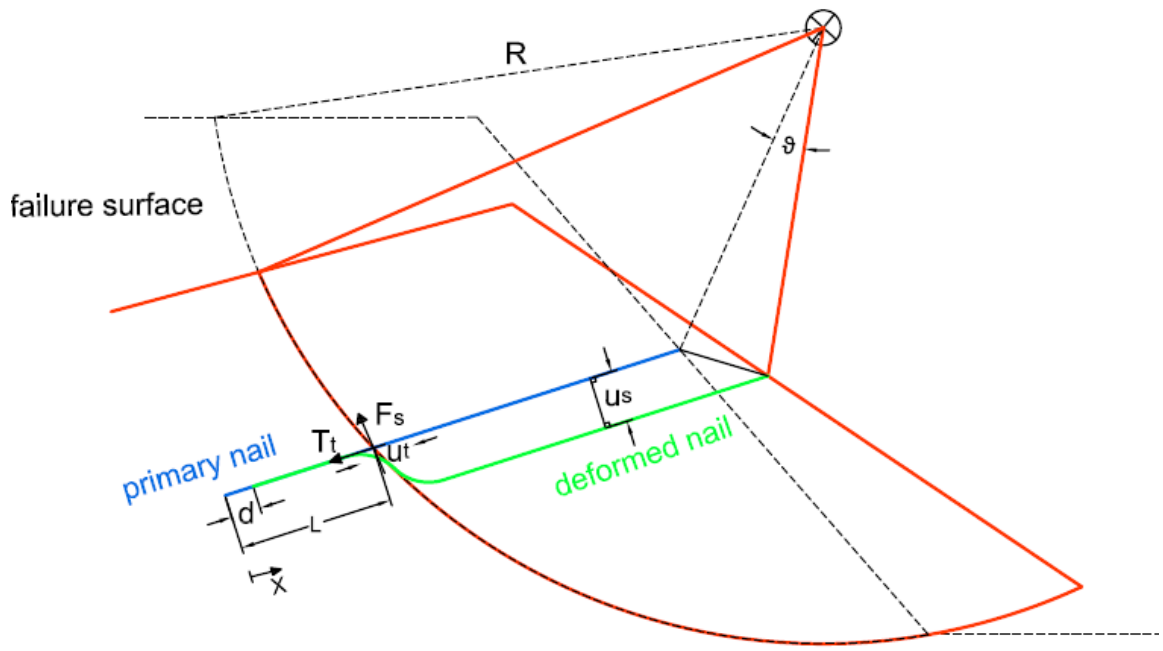

Figure 2.9. Relative displacements and resisting forces mobilized in the nail.

(1) For case I: $u_t < u_p$ at $X = L$(BC's: $\varepsilon = 0$ at $X = 0$ & $u = u_t$ at $X = L$)

In this case, the magnitude of the mobilized displacement at the assumed failure surface is less than the magnitude of displacements causing peak shear stress at the interface of soil and nail.

The function satisfying Eq. (7-1) is as follows.

$$u = c_1 e^{ax} + c_2 e^{-ax} \tag{8}$$

Where, c_1 and c_2 are integral constants and $a = \sqrt{D\pi k / EA}$

Derivative of Eq. (8):

$$\frac{du}{dx} = c_1 a e^{ax} - c_2 a e^{-ax} \tag{9}$$

By putting the boundary condition ($x = 0 : \varepsilon = du/dx = 0 \; and \; x = L : u = u_t$) into Eq. (8) & (9), following equations are obtained:

$$@\, x = 0 : \varepsilon = 0 \qquad \rightarrow \qquad c_1 = c_2$$

$$@\ x = L:\ u = u_t \qquad \rightarrow \qquad c_1 = \frac{u_t}{2\cosh(aL)}$$

$$u = \frac{u_t}{\cosh(aL)}\cosh(ax) \qquad\qquad 0 < x \leq x_p$$

(10-1)

$$\tau = ku = \frac{ku_t}{\cosh(aL)}\cosh(ax)$$

(10-2)

$$\mathrm{T} = \int_0^x D\pi\tau dx = \frac{D\pi k u_t}{\mathrm{a}\cosh(aL)}\sinh(ax)$$

(10-3)

$$@x = L: \qquad T_t = \frac{D\pi k}{a}\tanh(aL)\,.\,u_t = \sqrt{EAD\pi k}\,\tanh(aL)\,.\,u_t$$

(10-4)

(2) For case II: $u_t > u_p$ at $X = L$ (BC's: $x = x_p : u = u_p \; and \; T = T_0$)

The X_p, is the position in which the peak frictional stress starts to develop.

The function satisfying Eq. (7-2) is as follows.

$$u = \frac{D\pi\tau_p}{2S}x^2 + Ax + B \qquad\qquad x_p < x \leq L$$

(11)

$$\frac{du}{dx} = \frac{D\pi\tau_p}{S}x + A$$

(12)

Where, A and B are constants

For the case $x = x_p$ in Eq. (10-3)

$$T_0 = \frac{D\pi k u_p}{\mathrm{a}}\tanh(ax_p)$$

(13)

Constant A is obtained by putting $x = x_p$ into Eq. (12) and derivative of Eq. (10-1), in addition by applying $(x = x_p : u = u_p)$ to Eq. (11), constant B is determined and following equations can be achieved.

$$u = \frac{D\pi\tau_p}{2S}\left(x - x_p\right)^2 + a\,u_p \tanh(ax_p)\left(x - x_p\right) + u_p \qquad x_p < x \le L$$

(14)

Combining Eq. (13) with Eq. (14) we obtain

$$u = \frac{D\pi\tau_p}{2S}\left(x - x_p\right)^2 + \frac{T_0}{S}\left(x - x_p\right) + u_p$$

(15-1)

$$T = T_0 + \int_{x_p}^{x} D\pi\tau_p dx = T_0 + D\pi\tau_p(x - x_p)$$

(15-2)

The tensile force developed at $x = L$ can be obtained as follows.

$$T_t = \sqrt{EAD\pi k}\,\tanh\left(ax_p\right)u_p + D\pi\tau_p\left(L - x_p\right)$$

(15-3)

Thus the distribution of relative displacements, frictional stresses and tensile forces acting any part of reinforced soil can be obtained by suing Eqs. (10) and (15) as schematically in figure 2.10.

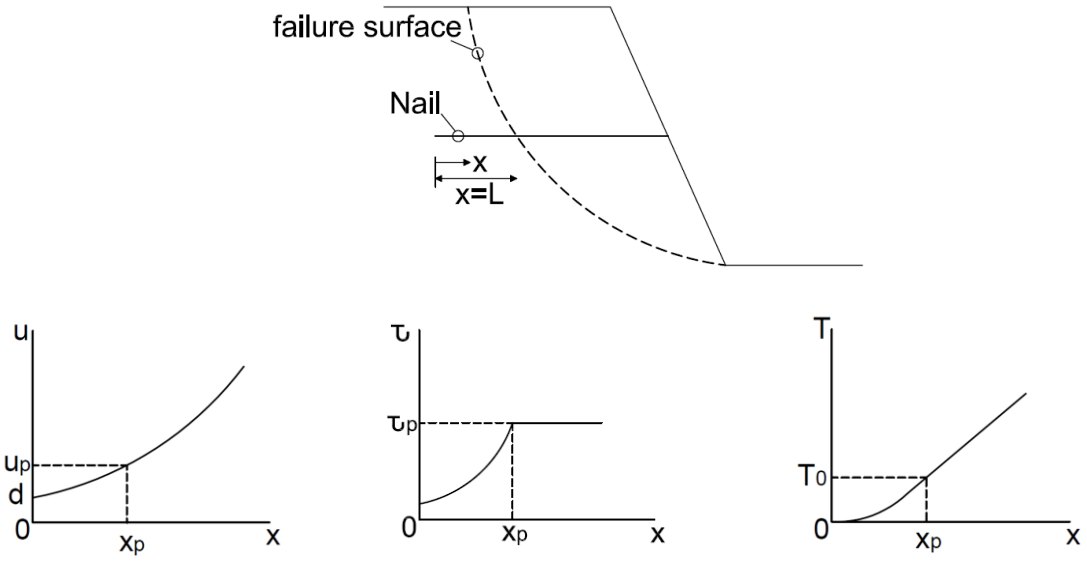

Figure 2.10. Distribution of relative displacement, frictional stress and tensile force along the nail (Mitachi et al.1992).

Furthermore, the relative displacement at $x = L$ can be calculated by:

$$u_t - u_p = \frac{T_t}{EA} - \int_0^l \frac{D\pi\tau_p x}{EA}\,dx$$

$$= \frac{(L - x_p)}{EA}\sqrt{EAD\pi k}\tanh(ax_p)\,u_p + \frac{D\pi\tau_p(L - x_p)^2}{2EA} \quad (16)$$

Where $l = L - Xp$**.** Then, the value of x_p can be obtained by a numerical method provided that the value of u_t is given.

Mitachi et al. (1992) showed that $u = 0$ does not exist means that irrespective of the length of nail, frictional resistances acting along the entire length of nail. The axial force in the nail decreases toward the rear end of nail, and therefore it should be considered that the rear end of nail moves even if it is microscopically small. And the required embedment length should be determined by taking allowable rear end displacement into consideration (Kim et al. 1997).

2.4.3 Shear force

The shear stress mobilized in the soil nail is determined by considering the equation of an elastic bending of the inclusion. Theoretically the soil nail is considered as infinitely long, and then the solution for the maximum shear force (F_s) mobilized at the intersection with failure surface is calculated as

$$F_s = 2\,E\,I\,\lambda^3 u_s \quad (17)$$

Where $\lambda = 4\sqrt{k_s D/(4EI)}$, k_s = modulus of lateral soil reaction, D = diameter of the nail, EI = bending stiffness of the nail and u_s = displacement normal to the direction of nail length (Kim et al. 1997).

2.5 Limit Equilibrium Slope Stability Methods

2.5.1 Background and history

Limit equilibrium types of analyses for evaluating the stability of slopes have been used in geotechnical engineering for many years. In the 20th century the idea of discretizing a

potential sliding mass into vertical slices was founded and is consequently one of the oldest numerical analysis technique in geotechnical engineering.

In 1916, Petterson (1955) presented the stability analysis of the Stigberg Quay in Gothenberg, Sweden and assumed that the slip surface is circular and the sliding mass was divided into slices. During the next decades, Fellenius (1936) introduced the Ordinary method of slices. In the mid-1950s Janbu (1954) and Bishop (1960) developed advances in the method. The advent of computers in the 1960s, handling the iterative procedures became easy which led to the mathematically more accurate formulations such as those developed by Morgenstern and Price (1965) and by Spencer (1967).

Limit equilibrium formulations according to the method of slices are also being applied to the stability analysis of structures such as nail reinforced slopes, tie-back walls and the sliding stability of structures subjected to high horizontal loading arising.

2.5.2 Method basics

Some different solution techniques for the method of slices have been developed over the years. Primarily, all are very similar. The differences between the methods are which including and satisfying equations of statics, which including interslice forces and what is the assumed relationship between the interslice shear and normal forces. Figure 2.11 shows a typical sliding mass divided into slices and the possible forces on the slice. Normal and shear forces act on the slice base and on the slice sides (Krahn 2012).

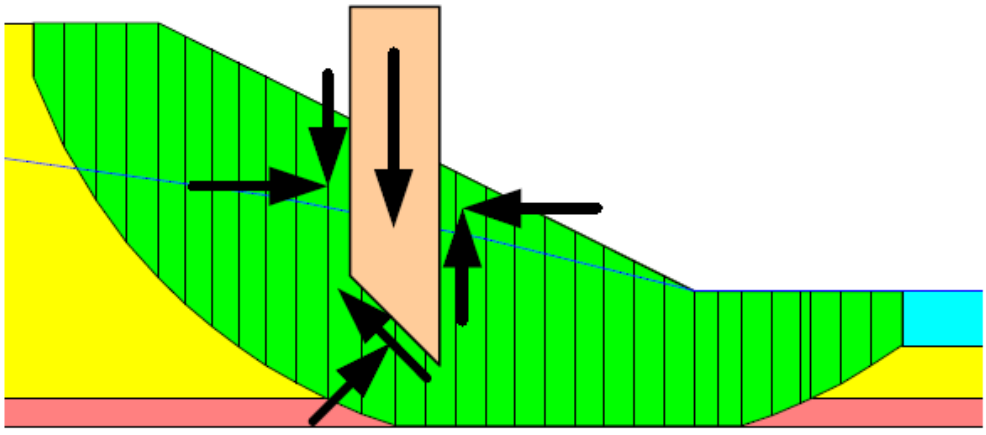

Figure 2.11. Slice discretization and slice forces in a sliding mass (Krahn 2012).

The Ordinary, or Fellenius method ignored all interslice forces and satisfied only moment equilibrium as the first method developed. Using these simplified assumptions made it possible to compute a factor of safety using hand calculations.

Later Bishop (1960) developed a method that included interslice normal forces, but ignored the interslice shear forces. Bishop's Simplified method satisfies only moment equilibrium. This method by including the normal interslice forces proposed this fact that the factor of safety equation turned into nonlinear and an iterative procedure was necessary to calculate the factor of safety.

The Janbu's simplified and the Bishop's Simplified methods are quite the same as in both the normal interslice forces included and the interslice shear forces ignored. The difference between them is that the Janbu's Simplified method satisfies only horizontal force equilibrium.

Later, computers made it possible to easily handle the iterative procedures in the limit equilibrium method, this lead to mathematically more accurate formulations which include all interslice forces and satisfy all equations of statics such as Morgenstern_Price and Spencer methods.

Table 2-1 lists the methods and indicates what static equations are satisfied for each of the methods. Table 2-2 gives a summary of the interslice forces included and the assumed relations between the interslice shear and normal forces.

Table 2-1 Equations of Statics Satisfied (Krahn 2012)

Method	Moment Equilibrium	Force Equilibrium
Ordinary or Fellenius	Yes	No
Bishop's Simplified	Yes	No
Janbu's Simplified	No	Yes
Spencer	Yes	Yes
Morgenstern-Price	Yes	Yes
Corps of Engineers – 1	No	Yes
Corps of Engineers – 2	No	Yes
Lowe-Karafiath	No	Yes
Janbu Generalized	Yes (by slice)	Yes
Sarma – vertical slices	Yes	Yes

Table 2-2 Interslice force characteristics and relationships (Krahn 2012)

Method	Interslice Normal (E)	Interslice Shear (X)	Inclination of X/E Resultant, and X-E Relationship
Ordinary or Fellenius	No	No	No interslice forces
Bishop's Simplified	Yes	No	Horizontal
Janbu's Simplified	Yes	No	Horizontal
Spencer	Yes	Yes	Constant
Morgenstern-Price	Yes	Yes	Variable; user function
Corps of Engineers – 1	Yes	Yes	Inclination of a line from crest to t
Corps of Engineers – 2	Yes	Yes	Inclination of ground surface at top of slice
Lowe-Karafiath	Yes	Yes	Average of ground surface and slice base inclination
Janbu Generalized	Yes	Yes	Applied line of thrust and moment equilibrium of slice
Sarma – vertical slices	Yes	Yes	$X = C + E \tan \varphi$

2.5.3 Definition of variables (Factor of safety)

The factor of safety is a factor that reduces the shear strength of the soil to bring the soil mass into a limiting equilibrium state along the desired slip surface.

For effective stress analysis, the shear strength is defined as:

$$s = c' + (\sigma_n - u) \tan \phi' \tag{18}$$

Where (all the variables are defined as in (Krahn 2012)):

s = Shear strength,

c' = Effective cohesion,

ϕ' = Effective angle of internal friction,

σ_n = Total normal stress, and

u = Pore-water pressure.

For a total stress analysis, the resistance parameters are determined in terms of total stresses and pore-water pressures are not needed.

The stability analysis includes passing a slip surface through the earth mass and dividing the inscribed portion into vertical slices. The slip surface may be circular, composite (i.e.,

combination of circular and linear portions) or consist of any shape defined by a series of straight lines (i.e., fully specified slip surface) (Krahn 2012).

As mentioned by Krahn (2012) the limit equilibrium formulation presume that:

- The factor of safety of the cohesive component of strength and the frictional component of strength are mobilized in the same relation for all soil layers involved
- The factor of safety is the same for all slices.

Figure 2.12 shows all the forces acting on a circular slip surface. The variables are defined as follows (all the variables are defined as in Krahn (2012)):

W = The total weight of a slice of width b and height h.

P = The total normal force on the slice base.

S_m = The shear force mobilized on the base of each slice.

E = The horizontal interslice normal forces. Subscripts L and R designate the left and right sides of the slice, respectively.

X = The vertical interslice shear forces. Subscripts L and R define the left and right sides of the slice, respectively.

R = The radius for a circular slip surface.

x = The horizontal distance from the centerline of each slice to the center of rotation or to the center of moments.

h = The vertical distance from the center of the base of each slice to the uppermost line in the geometry (i.e., generally ground surface).

a = The perpendicular distance from the resultant external water force to the center of rotation or to the center of moments. The L and R subscripts designate the left and right sides of the slope, respectively.

A = The resultant external water forces. The L and R subscripts designate the left and right sides of the slope, respectively.

θ = The angle between the tangent to the center of the base of each slice and the horizontal. The sign convention is as follows. When the angle slopes in the same direction as the overall slope of the geometry, α is positive, and vice versa.

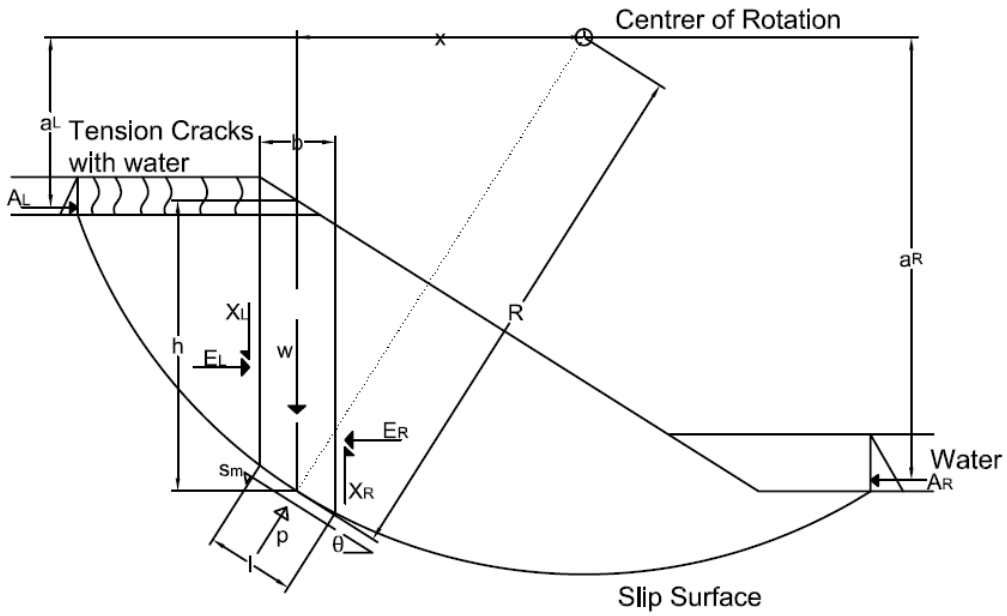

Figure 2.12. Forces acting on a slice through a sliding mass with a circular slip surface (Krahn 2012).

The magnitude of the shear force mobilized to satisfy conditions of limiting equilibrium is:

$$S_m = \frac{l\,S}{F} = \frac{l}{F}(c' + (\sigma_n - u)tan\varphi') \tag{19}$$

$\sigma_n \quad = {}^{P}/_{l} =$ Average normal stress at the base of each slice

$F \quad =$ The factor of safety

$l \quad =$ The base length of each slice

The summations of forces in two directions and the summation of moments which are known as the elements of statics, can be used to derive the factor of safety. However, the elements of statics, along with failure criteria, are insufficient to solve the problem. More information is necessary about either the normal force distribution at the base of the slices or the interslice force distribution. Table 2-3 and Table 2-4 summarize the known and unknown quantities associated with a slope stability analysis (Krahn 2012).

Table 2-3 Summary of known quantities in solving for a safety factor (Krahn 2012)

Number of Known Quantities	Description
n	Summation of forces in the horizontal direction
n	Summation of forces in the vertical direction
n	Summation of moments
n	Material Shear Failure Criterion
4n	Total number of equations

Table 2-4 Summary of unknown quantities in solving for a safety factor (Krahn 2012)

Number of Unknown Quantities	Description
n	Magnitude of the normal force at the base of a slice, N
n	Point of application of the normal force at the base of each slice
n - 1	Magnitude of the interslice normal forces, E
n - 1	Magnitude of the interslice shear force, X
n - 1	Point of application of the interslice forces
n	Shear force on the base of each slice, Sm
1	Factor of safety, F
1	Value of Lambda, λ
6n - 1	Total number of unknowns

Since the number of unknown quantities is more than the number of known quantities, the problem is indistinctive. To make the problem determinate, some assumptions concerning the magnitude, directions, and/or point of application of some of the forces must be done. The first assumption in most methods is the point of application of the normal force at the base of a slice that acts through the centerline of the slice. Then an assumption is most commonly made regarding the magnitude, direction, or point of application of the interslice forces.

In overall, the various methods of slices can be classified in terms of:

- The statics used in determining the factor of safety equation, and
- The interslice force assumption used to solve the problem.

General limit equilibrium method

As it is well explained by Krahn (2012) the General Limit Equilibrium method (GLE) uses the following equations of statics in solving for the factor of safety:

- To calculate the normal force at the base of the slice, N, the summation of forces in a vertical direction for each slice is applied.
- To calculate the interslice normal force, E, the summation of forces in a horizontal direction for each slice is used. This equation is applied in an integration manner across the sliding mass (i.e., from left to right).
- The summation of moments about a common point for all slices. The equation can be rearranged and solved for the moment equilibrium factor of safety, F_m.
- The summation of forces in a horizontal direction for all slices, giving rise to a force equilibrium factor of safety, F_f.

Since the analysis is still indeterminate, further assumption must be made concerning the direction of the outcome interslice forces. The direction is assumed to be characterized by an interslice force function. The direction along with the interslice normal force is utilized to compute the interslice shear force. Thereafter, the factors of safety can now be computed based on force equilibrium (F_f) and moment equilibrium (F_m). These factors of safety can be varied relying on the percentage (λ) of the force function used in the computation. The factor of safety providing both moment and force equilibrium is recognized to be the converged factor of safety of the GLE method.

It is also feasible to specify a variety of interslice force conditions and satisfy only the moment or force equilibrium conditions using the same GLE approach. The assumptions made to the interslice forces and the selection of overall force or moment equilibrium in the factor of safety equations, lead to the various methods of analysis (Krahn 2012).

Moment equilibrium factor of safety

To obtain the moment equilibrium factor of safety equation, reference can be made to figure 2.12. In every case, the summation of moments for all slices can be written as follows:

$$\Sigma W x \; - \; \Sigma S_m R \; \pm \; \Sigma A a \; = \; 0$$

(20)

After substituting for S_m and rearranging the terms, the factor of safety with respect to moment equilibrium is:

$$F_m = \frac{\sum[c'l + (P - ul)\tan\phi']R}{\sum Wx \pm Aa}$$

(21)

This equation is a nonlinear equation since the normal force P is also a function of the factor of safety (Krahn 2012).

Force equilibrium factor of safety

Again, reference can be made to figure 2.12 to derive the equation of force equilibrium factor of safety. The summation of forces in the horizontal direction for all slices is:

$$\sum(\mathrm{E}_L - \mathrm{E}_R) - \sum(S_m \times \cos(\theta)) + \sum(\mathrm{P} \times \sin(\theta)) \pm \sum A = 0$$

(22)

The term $\sum(\mathrm{E}_{Li} - \mathrm{E}_{Ri})$ presents the interslice normal forces and must be zero when summed over the entire sliding mass. After substituting for S_m and rearranging the terms, the factor of safety with respect to horizontal force equilibrium is:

$$F_f = \frac{\sum[c'l + (P - ul)\tan\phi']\cos\theta}{\sum P\sin\theta \pm A}$$

(23)

Slice normal force at the base

The normal force at the base of a slice is derived from the summation of forces in a vertical direction on each slice.

$$\mathrm{X}_L - \mathrm{X}_R + \mathrm{W} - S_m \times \sin(\theta) - \mathrm{P} \times \cos(\theta) = 0$$

(24)

Once again, after substituting for S_m the equation for the normal force at the base of each slice is:

$$P = \frac{W + (\mathrm{X}_L - \mathrm{X}_R) - \frac{c'l\sin\theta}{F} + \frac{ul\tan\phi'\sin\theta}{F}}{\cos\alpha + \frac{\sin\alpha\tan\phi'}{F}}$$

(25)

The equation for the normal force is nonlinear, with the value dependent on the factor of safety, F. The factor of safety is equal to the moment equilibrium factor of safety, F_m, when solving for moment equilibrium, and equal to the force factor of safety, F_f, when solving for force equilibrium.

Since the factor of safety (F) and the interslice shear forces, (i.e., X_L and X_R) are unknown, the base normal equation cannot be solved directly. Consequently, P needs to be determined using an interactive scheme.

To solve the factor of safety, at first the interslice shear and normal forces are ignored and the normal force on each slice can be calculated directly by summing forces in the same direction as the normal force.

$$P = W\ cos\theta$$

(26)

To obtain commencing values for the factor of safety calculations, we can use this simplified normal equation which is known as Fellenius or Ordinary method factor of safety.

If we ignore the interslice shear forces, but retain the interslice normal forces, then the slice base normal force equation is

$$P = \frac{W - \frac{c'l\sin\theta}{F} + \frac{ul\tan\phi'\sin\theta}{F}}{\cos\alpha + \frac{\sin\alpha\tan\phi'}{F}}$$

(27)

If we use this equation for the base normal, Janbu Simplified factor of safety is the factor of safety with respect to force equilibrium. And the factor of safety according to moment equilibrium is the Bishop simplified factor of safety (Krahn 2012).

Interslice forces

The interslice forces are defined as the normal and shear forces appearing in the vertical faces between slices. The interslice normal forces are determined using an integration procedure starting at the left end of each slip surface.

The summation of forces in a horizontal direction can be written for each slice as:

$$\mathrm{E}_L - \mathrm{E}_R - S_m \times \cos(\theta) + \mathrm{P} \times \sin(\theta) = 0$$

(28)

Substituting S_m in this and then solving for the interslice normal on the right side of each slice gives:

$$\mathrm{E}_R = \mathrm{E}_L - \frac{(c'l - ul\tan\phi')\cos\theta}{F} + \mathrm{P} \times (\sin\theta - \frac{\tan\phi'\cos\theta}{F}) = 0$$

(29)

Because the left interslice normal force of the first slice is zero (i.e., $E_L = 0$) , the interslice normal force of all slices can be calculated. It is noticeable that the equation for computing the interslice normal force is relying on the factor of safety and it is renewed through the iteration process.

Thanks to empirical equation proposed by Morgenstern and Price (1965) the interslice shear force can be calculated as a percentage of the interslice normal force, once the interslice normal force is known:

$$X = E\lambda\, f\,(x)$$

(30)

where:

λ = The percentage (in decimal form) of the function used, and

$f(x)$ = Interslice force function representing the relative direction of the resultant interslice force.

Figure 2.13 shows some typical function shapes. The type of force function used in calculating the factor of safety is the prerogative of the user.

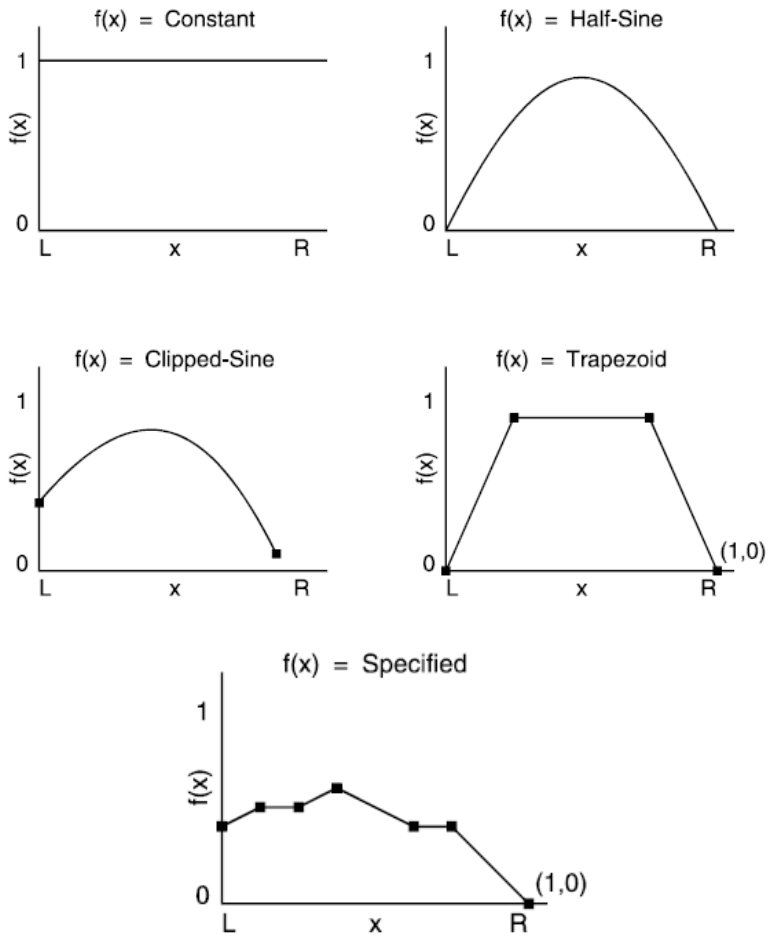

Figure 2.13. Example interslice force functions (Krahn 2012)

Slope stability with nails

In this section, the stability of nailed slopes is discussed with the modified equilibrium equations incorporating the effect of soil nails. In the present analysis not only nail tension is considered but also shear force of soil nails is included in the moment and force equilibrium formulation. Tensile and shear forces mobilized in the nail are calculated in previous sections.

Bishop Method

As mentioned earlier, method of slices with circular failure surface is employed in this method for analyzing stability of nailed slope. Only those nail tensile forces are considered in the equilibrium equations of the slices which are from the reinforcements emerging out of the base of the slices. Forces acting on a typical slice are presented in figure 2.14.

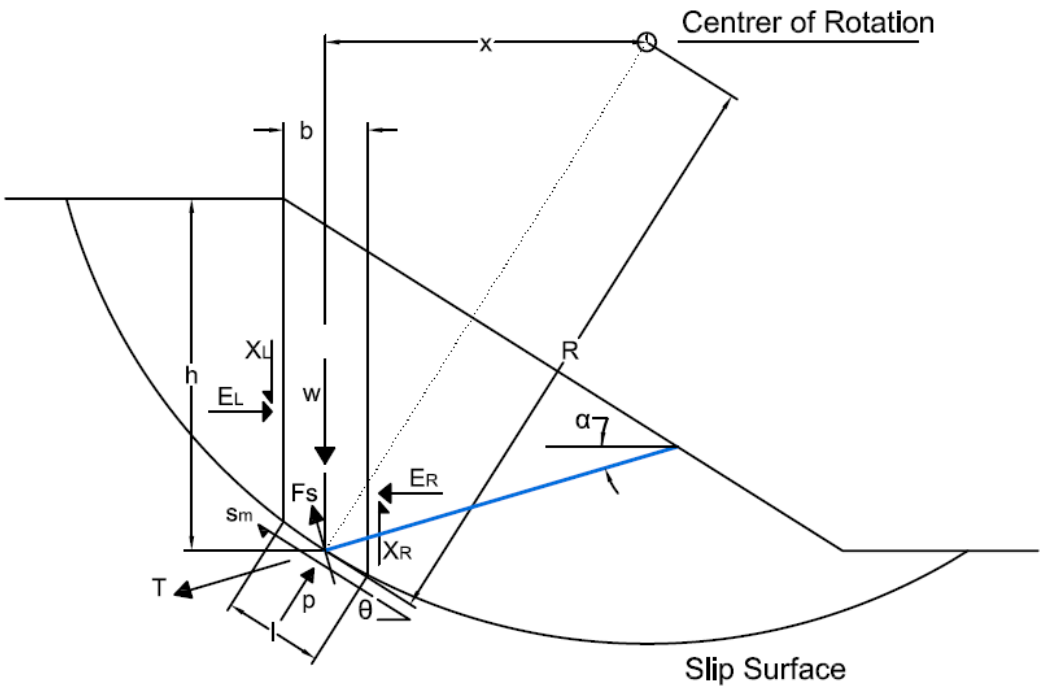

Figure 2.14 applied forces on a slice including nail tension and shear force

Where (the variables are defined as in Krahn (2012)),

W = The total weight of a slice of width b and height h

P = The total normal force on the base of the slice

S_m = The shear force mobilized on the base of each slice.

E = The horizontal interslice normal forces. Subscripts L and R designate the left and right sides of the slice, respectively.

X = The vertical interslice shear forces. Subscripts L and R define the left and right sides of the slice, respectively.

R = The radius for a circular slip surface.

h = The vertical distance between the center of the base of each slice to the uppermost line in the geometry (i.e., generally ground surface).

l = The base length of each slice.

θ = The angle between the tangent to the center of the base of each slice and the horizontal.

α = The angle of nail with horizontal

T = Nail tensile force for the reinforcement emerging out from the slice base

F_s = Shear force of nail mobilized at the intersection with failure surface

F = The factor of safety

Considering overall moment equilibrium of the forces acting on each slice is given by

$$\sum WR\sin\theta - \sum S_m R - \sum TR\cos(\alpha+\theta) - \sum F_s R\sin(\alpha+\theta) = 0 \tag{31}$$

Replacing Eq. (19) in Eq. (31) and rearranging

$$F = \frac{\sum lc' + \sum P\ \tan\phi' + F\sum T\ \cos(\alpha+\theta) + F\sum F_s\sin(\alpha+\theta)}{\sum W\sin\theta} \tag{32}$$

From vertical force equilibrium of each slice

$$\sum F_v = P\cos\theta + F_s\cos\alpha + S_m\sin\theta - W - T\sin\alpha = 0 \tag{33}$$

Replacing Eq. (19) in Eq. (33) and rearranging

$$P = \frac{W + T\sin\alpha\ - \frac{l}{F}c'\sin\theta - F_s\cos\alpha}{\cos\theta + \frac{\tan\phi'\sin\theta}{F}} \tag{34}$$

Combining Eq. (32) with Eq. (34)

$$F = \frac{\sum\frac{1}{m_a}(lc'\cos\theta + (W + T\sin\alpha\ - F_s\cos\alpha)\tan\phi' + F\sum T\ \cos(\alpha+\theta) + F\sum F_s\sin(\alpha+\theta)}{\sum W\sin\theta} \tag{35}$$

Where

$$m_a = \cos\theta + \frac{\tan\phi'\sin\theta}{F} \tag{36}$$

Spencer Method

Similar assumptions are also applied in this method for calculating stability of nailed slopes. As mentioned earlier, the method includes all interslice forces and satisfy all equations of statics. Forces acting on a typical slice are the same as in Bishop Method, as given in figure 2.14.

As derived in the previous case, the normal force obtained from the vertical equilibrium of the slice is given by

$$P = \frac{W + T\sin\alpha\ - \frac{l}{F}c'\sin\theta - F_s\cos\alpha - \ X_R + X_L}{\cos\theta + \frac{\tan\phi'\sin\theta}{F}}$$

(37)

In case of an individual slice i, the horizontal force equilibrium equation is given by

$$E_R - E_L + F_s\sin\alpha + T\cos\alpha - P\sin\theta + S_m\cos\theta = 0$$

(38)

The term $\sum(\mathrm{E}_{Li} - \mathrm{E}_{Ri})$ presents the interslice normal forces and must be zero when summed over the entire sliding mass. By replacing Eq. (19) in Eq. (38) and rearranging the equation, following factor of safety with respect to the force equilibrium may be obtained

$$F_f = \frac{\sum(lc' + P\tan\phi')\cos\theta + F\sum(F_s\sin\alpha + T\cos\alpha)}{\sum P\sin\theta}$$

(39)

Similar to the previous method, factor of safety with respect to moment equilibrium can be solved

$$F_m = \frac{\sum(lc' + P\tan\phi') + F\sum F_s\sin(\alpha+\theta) + F\sum T\cos(\alpha+\theta)}{\sum W\sin\theta}$$

(40)

3 Analytical Coding

3.1 Introduction

MATLAB is an interpreted language with dynamic, inferenced types. It is a high-level language with nice syntax for performing matrix operations, and has many high-performance matrix math libraries built-in.

This thesis proposes an analytical code programing by MATLAB software. It describes the evolution of resisting forces along the nail regarding to relative displacement between soil and nail in the process of the failure of a slope.

The analytical code has been developed to simulate a specified soil nail reinforced slope. It is able to estimate values of tensile and shear forces mobilized in each reinforcement regarding to specified relative displacement between soil and nail by considering different parameters, such as the soil shear modulus, the nail dimensions and elastic modulus of the nail.

The program makes it possible to analyze the slope stability reinforced with nails by using Bishop and Spencer Methods and finally to compare the values of factor of safeties with respect to different relative displacements between soil and nail.

3.2 Definition of parameters

At first we should specify the input parameters to define the geometry of slope and estimate the material parameters to calculate the key variables to obtain resisting forces mobilized in the nails and consequently to compute Factor of safety by using Bishop and Spencer methods. Parameters of the slope are presented in figure 3.1.

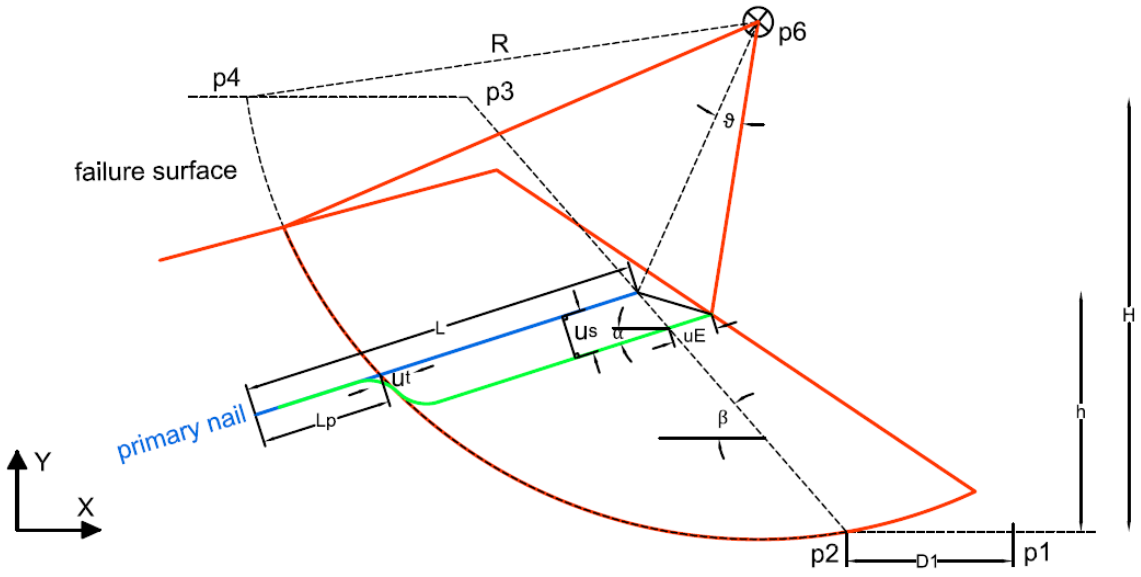

Figure 3.1. Slope parameter specifications

Input variables are defined as follows:

Slope parameters

$p1$ = Desired start point to draw the slope ($[100,0]$)

$p2$ = The point which specifies toe of the slope

$p3$ = The point which specifies top of the slope

$p4$ = The point which specifies top of the circular slip surface

$p6$ = The point which specifies center of the circular slip surface

$D1$ = Horizontal distance between $p2$ and $p1$

H = Height of the slope

$betta$ = Slope angle

$gamma$ = Specific weight of soil

$cohesion$ = Cohesion of soil

phi = Angle of internal friction

$tetta$ = Slope rotation angel

Nail parameters

L = Soil-nail length

Lp = Passive length of the nail

Ds = Diameter of steel

Dc = Diameter of nail hole

h = Vertical distance of the nail head from the ground

$alpha$ = Angle of soil-nail below the horizontal

Es = Elastic modulus of the steel

tp = Peak shear stress at the interface of soil and nail

up = Soil-nail displacement causing peak shear stress

Ksh = Modulus of lateral soil reaction

$Fshmax$ = Peak shear force

ut = Displacement between soil and nail in the direction of nail length at the distance of Lp from the nail tip

uE = The length of the nail that is pulled out from the slope face

Matrixes which describe the input data:

$inputdata = [D1, H, betta, gamma, cohesion, phi]$

$naildata = [L, Ds, Dc, h1, h2, \dots hn, alpha, Es, tp, up, Ksh, Fshmax]$

$h1\ h2 \dots hn$ specify the vertical distances of nails' head from the ground

To draw a simple slope and soil-nails following terms are defined:

Number of nails is calculated as follow

$$nnail = length(naildata) - 9$$

Where

- $length(naildata)$ refers to the number of elements of matrix $naildata$
- Number 9 refers to the number of elements of matrix $naildata$ without $h1\ h2 \dots hn$

$nails = zeros(nnail, 4)$

Nails head height, passive length Lp, displacements uE and ut for each nails will be calculated and placed as the elements of matrix $nails = [\text{height}, \text{Lp}, \text{uE}, \text{ut}]$. Each array belongs to parameters of one nail.

$a1 = naildata(1, length(naildata) - 5) \times pi/180$

$a1$ describes orientation of soil-nail below the horizontal in radian

A = Section area of steel nail = $pi \times Ds\text{^}2/4$

Ist = Second moment area of steel nail = $pi/64 * Ds\text{^}4$

Length and width of rectangular area which contains center of circular slip surface are assumed as follow

l = Length of the rectangle = $0.4 \times max(H/tan(betta), H)$

b = Width of the rectangle = $0.6 \times min(H/tan(betta), H)$

Position of slope points

In the figure 3.2 slope points are specified

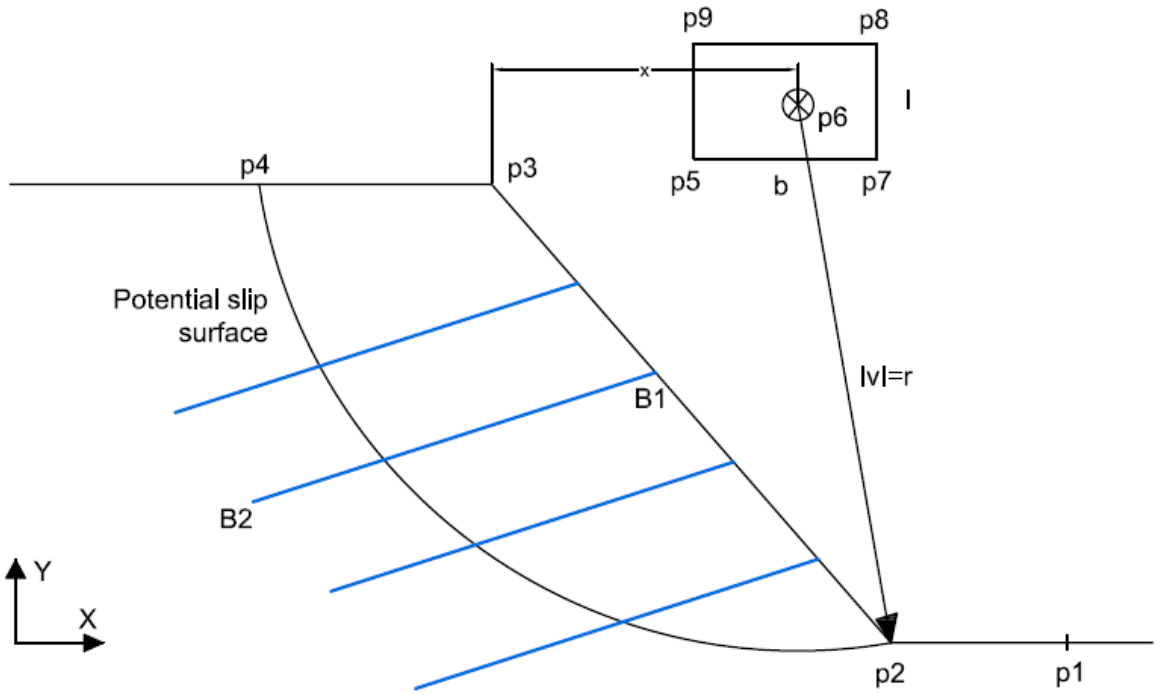

Figure 3.2. Slope point specifications

$p1 = [100; 0]$

$p2 = [p1(1) - D1; 0]$

$p3 = [p1(1) - (D1 + H/tan(betta)); H]$

Position of nails' points

Matrix $nailp$ includes position of head and tip of nails $B1(x, y), B2(x, y)$

$nailp = [B1x, B1y, B2x, B2y]$

$= [p2(1) - \frac{nails(:,1)}{tan(betta)}, p2(2) + nails(:,1), p2(1) - \frac{nails(:,1)}{tan(betta)} - L1 * cos(a1), p2(2) + nails(:,1) - L1 * sin(a1)]$

To specify point $p5$ we considered two conditions:

$$\begin{cases} betta > 45 & \mathrm{p5} = \left[\mathrm{p2}(1) + 2.2; \mathrm{H} + 0.51 * \min\left(\dfrac{\mathrm{H}}{\tan(\mathrm{betta})}, \mathrm{H}\right)\right] \\ betta \leq 45 & \mathrm{p5} = \left[\mathrm{p2}(1) - 2.5 * \dfrac{\dfrac{\mathrm{H}}{\tan(\mathrm{betta})}}{6}; \mathrm{H} + 0.5 * \min\left(\dfrac{\mathrm{H}}{\tan(\mathrm{betta})}, \mathrm{H}\right)\right] \end{cases}$$

Following matrixes return to the rectangular area

$p7 = [p5(1) + b; p5(2)]$

$p8 = [p7(1); p5(2) + l]$

$p9 = [p5(1); p5(2) + l]$

$p6$ = Center point of circular slip surface = $p5 + [2 * (b/4);\ 2 * (l/4)]$

3.3 Plotting the soil nailed slope

To draw the slip surface we can plot a part of a circle (arc) when begin point, end point and center point of the circle are known.

1. Circular slip surface radius

   v = Radius vector = $p2 - p6$

   r = Radius = $norm(v)$

2. To control if the center point is placed in a proper position it means if the horizontal distance between center point $p6$ and $p3$ is less than the radius of slip surface

   x = Horizontal distance between $p6$ and $p3 = sqrt(r\text{^}2 - (H - p6(2))\text{^}2)$

   $x > (p6(1) - p3(1))$

3. Drawing slip circular surface

   $p4 = [p6(1) - x; H]$

   $x1 = p4(1)$

   $y1 = p4(2)$

   $x2 = p2(1)$

   $y2 = p2(2)$

   $d = sqrt((x2 - x1)\text{^}2 + (y2 - y1)\text{^}2)$

   $a = atan2(-(x2 - x1), (y2 - y1))$

   $B = asin(d/2/r)$

$$c = linspace(a - B, a + B)$$

$$e = sqrt(r\text{^}2 - d\text{^}2/4)$$

$$x = (x1 + x2)/2 - e * cos(a) + r * cos(c)$$

$$y = (y1 + y2)/2 - e * sin(a) + r * sin(c)$$

Plot $(x, y, 'b', x1, y1, 'b', x2, y2, 'b', 'LineWidth', 1.5)$

Plotting the slices

For slope stability analysis we should divide the slip surface by number of desired slices. Figure 3.3 presents the specifications of slices. Here we assumed that all slices have the same width and made an assumption for width value:

$width = H/tan(betta)/4$

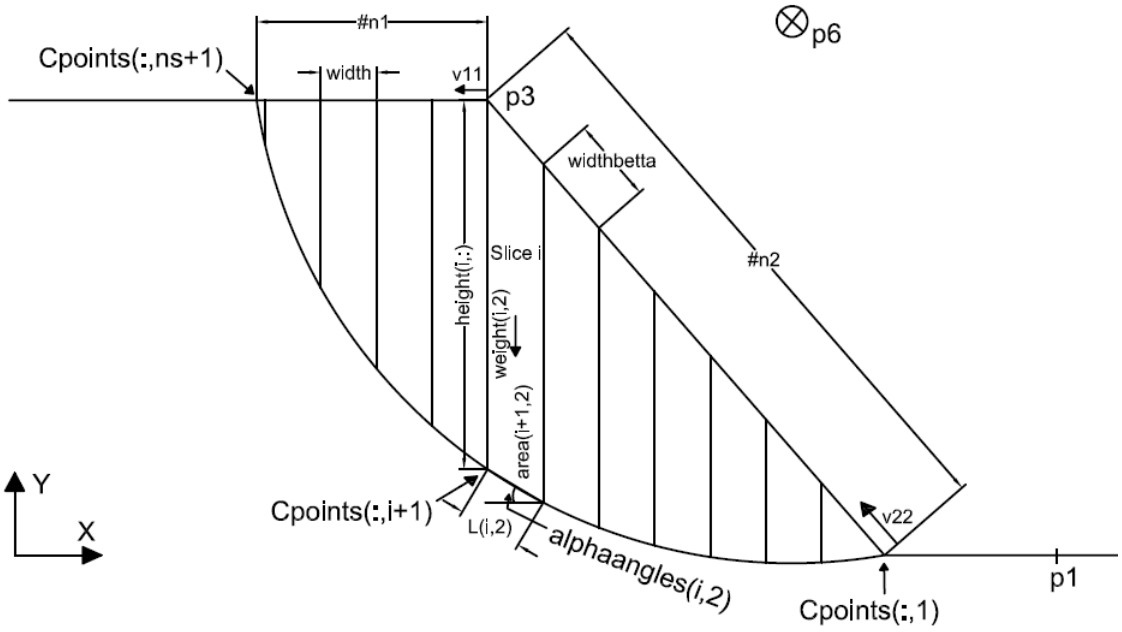

Figure 3.3. Slices specifications

Number of slices:

$$v1 = p4 - p3$$

$$n1 = floor(norm(v1)/width)$$

$$v2 = p3 - p2$$

$$widthbetta = width/cos(betta)$$

$$n2 = floor(norm(v2)/(widthbetta))$$

$$v11 = v1/norm(v1)$$

$C1 = p2$

$C2 = p3$

$v22 = v2/norm(v2)$

$ns = n1 + n2$

The determined value of base length of slices will be placed in the second column of matrix L, the first column specifies the number of slice.

$L = zeros(ns, 2)$

The coordinate of points which are result of cross of the slices with slip surface will be stored in matrix $Cpoints$.

$Cpoints = zeros(2, ns + 1)$

$Cpoints(:,1) = p2$

$Cpoints(:, ns + 1) = p4$

$alphaangles$ matrix will store the angle of slice bases to x-axis

$alphaangles = zeros(ns, 2)$

$height$ matrix will store the slice heights

$height = zeros(ns - 1,2)$

$area$ matrix will store the slice areas

$area = zeros(ns, 2)$

$weight$ matrix will store the weight of slice soil mass

$weight = zeros(ns, 2)$

$malpha$ matrix returns to Equation $m_a = \cos\theta + \frac{\tan\phi' \sin\theta}{F}$ which is required to determine factor of safety

$malpha = zeros(ns, 1)$

Right slices

for $i = 1{:}n2$ (from slice 1 to slice $n2$)

$C2 = p3 - (n2 - i) * widthbetta * v22$

$syms\ C11$ (To find the point which is result of crossing of arc line and slice)

$g1 = solve((C2(1) - p6(1))\text{^}2 + (C11 - p6(2))\text{^}2 - r\text{^}2, C11)$

By solving the equation, we have 2 answers that the first one is smaller than the second. For our problem the smaller one is the required answer.

$yg1 = g1(1)$ (Vertical distance of point $g1$ from the origin of coordinates)

Create the line of slices

line $([C2(1), C2(1)], [C2(2), yg1], 'Color', [1\ 0\ 1])$

$Cpoints(:, i+1) = [C2(1); yg1]$ (Point's coordinate)

$height(i, :) = [i; C2(2) - yg1]$ (Slice height)

for $i = 1{:}\, n2$ (from slice 1 to slice $n2$)

$baselengthvector = Cpoints(:, i+1) - Cpoints(:, i)$

$L(i, 1) = i$ (Slice number)

$L(i, 2) = norm(baselengthvector)$ (Length of the slice base)

$alphaangles(i, 1) = i$ (Slice number)

$alphaangles(i, 2) = atan2(Cpoints(2, i+1) - Cpoints(2, i), Cpoints(1, i+1) - Cpoints(1, i)) * 180/pi$ $(angle = atan2(y2 - y1, x2 - x1) * 180/pi)$

(Angle of the slice base from the horizontal)

$$\begin{cases} alphaangles(i,2) < -90 & alphaangles(i,2) = -180 - alphaangles(i,2) \\ alphaangles(i,2) > 90 & alphaangles(i,2) = 180 - alphaangles(i,2) \end{cases}$$

for $i = 1{:}\, (n2 - 1)$ (from slice 1 to slice $n2 - 1$)

$area(i + 1, 1) = i + 1$ $(slice\ number)$

$area(i + 1, 2) = (height(i, 2) + height(i + 1, 2)) * width/2$ (Slice area)

$C2 = p3$

Left slices

for $i = (n2 + 1){:}\, (ns - 1)$ (from slice $n2 + 1$ to slice $ns - 1$)

$C2 = C2 + width * v11$

$syms\ C22$ (To find the point which is result of crossing of arc line and slice)

$g2 = solve((C2(1) - p6(1))\text{^}2 + (C22 - p6(2))\text{^}2 - r\text{^}2, C22)$

By solving the equation, we have 2 answers that the first one is smaller than the second. For our problem the smaller one is the required answer.

$yg2 = g2(1)$ (Vertical distance of point $g2$ from the origin of coordinates)

Create the line of slices

line $([C2(1), C2(1)], [C2(2), yg2], 'Color', [1\ 0\ 1])$

$Cpoints(:, i+1) = [C2(1); yg2]$ (Points coordinates)

$baselengthvector = Cpoints(:, i+1) - Cpoints(:, i)$

$L(i, 1) = i$ (Slice number)

$L(i, 2) = norm(baselengthvector)$ (Length of the slice base)

$alphaangles(i, 1) = i$ (Slice number)

$alphaangles(i, 2) = atan2(Cpoints(2, i+1) - Cpoints(2, i), Cpoints(1, i+1) - Cpoints(1, i)) * 180/pi$ $(angle = atan2(y2 - y1, x2 - x1) * 180/pi)$ (Angle of the slice base from the horizontal)

$$\begin{cases} \text{alphaangles(i, 2)} > 90 & \text{alphaangles(i, 2)} = 180 - \text{alphaangles(i, 2)} \\ \text{alphaangles(i, 2)} \leq 90 & \text{alphaangles(i, 2)} = \text{alphaangles(i, 2)} \end{cases}$$

$height(i, 1) = i$ (Slice number)

$height(i, 2) = C2(2) - yg2$ (Slice height)

for $i = (n2 + 1): (ns - 1)$ (from slice $n2 + 1$ to slice $ns - 1$)

$area(i, 1) = i$ (Slice number)

$area(i, 2) = (height(i - 1, 2) + height(i, 2)) * width/2$ (Area of slices)

$L(ns, 1) = ns$ (Slice number ns)

$L(ns, 2) = norm(Cpoints(:, ns + 1) - Cpoints(:, ns))$ (base length of the slice ns)

$alphaangles(ns, 1) = ns$ (Slice number ns)

$alphaangles(ns, 2) = 180 - atan2(Cpoints(2, ns + 1) - Cpoints(2, ns), Cpoints(1, ns + 1) - Cpoints(1, ns)) * 180/pi$ (Angle of the slice base (number ns) from the horizontal)

$area(1,1) = 1$ (Slice number 1)

$area(1,2) = height(1,2) * L(1,2) * cos(alphaangles(1,2) * pi/180)/2$ (Area of slice 1)

$area(ns, 1) = ns$ (Slice number ns)

$area(ns, 2) = height(ns - 1,2) * L(ns, 2) * cos(alphaangles(ns, 2) * pi/180)/2$ (Area of slice ns)

for i=1:ns (From slice 1 to slice ns)

$weight(i, 1) = i$ (Slice number)

$weight(i,2) = area(i,2) * 1 * gamma$ (Weight of slice soil mass)

Displaying calculated values of base length of slices, base angle of slices from the horizontal and weight of slices soil mass in the matrix $data$

$data = [L(:,1)\ L(:,2)\ alphaangles(:,2)\ weight(:,2)]$

disp('slide base length base angle weight')

disp(data)

Nails specifications

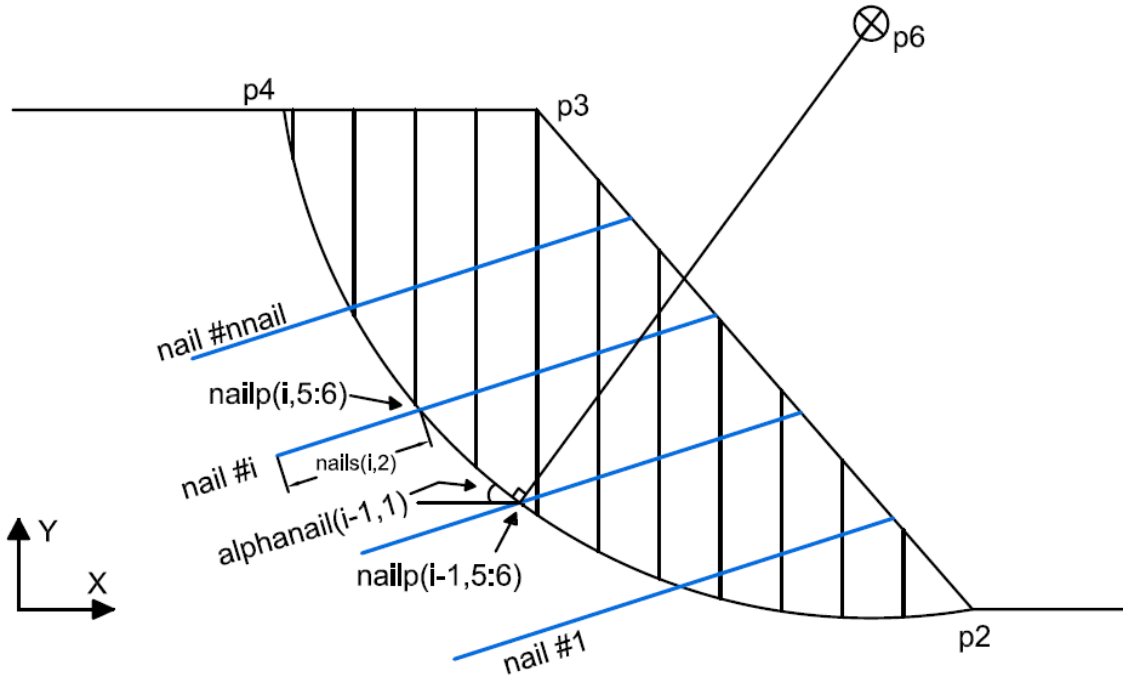

Figure 3.4. Nails specifications

Matrix $alphanail$ will store the angle of slice base which cross a nail ($nnail$ is the number of nails)

$alphanail = zeros(nnail, 1)$

for i=1:nnail (from the first nail to the last nail, $nnail$)

$syms\ Fx\ Fy$ (To find the point of the nail which cross the failure surface)

Circle equation:

$eqn1 = (Fx - p6(1))\text{^}2 + (Fy - p6(2))\text{^}2 - r\text{^}2$

$r =$ Radius of failure surface

Line/nail equation (Blue lines on figure 3.4.)

$$eqn2 = (nailp(i,2) - Fy) - tan(a1) * (nailp(i,1) - Fx)$$

$$(eqn2 = (B1(2) - Fy) - tan(a1) * (B1(1) - Fx))$$

When two lines meet each other:

$$answer = solve(eqn1, eqn2, Fx, Fy)$$

There are two answers:

$$gg = double(answer.Fx)$$

$$hh = double(answer.Fy)$$

The point where nail crosses the failure surface

$$\begin{cases} gg(1) < p2(1) & \text{nailp(i, 5: 6)} = [\text{gg(1)};\ \text{hh(1)}] \\ gg(1) \geq p2(1) & \text{nailp(i, 5: 6)} = [\text{gg(2)}; \text{hh(2)}] \end{cases}$$

Vector Lpp:

$$Lpp = [nailp(i,5); nailp(i,6)] - [nailp(i,3); nailp(i,4)]$$

Passive length Lp:

$$nails(i,2) = norm(Lpp)$$

To calculate the factor of safety equations we need to know the angle of slice base that includes nail ($alphanail$, figure 3.4.). Already we obtained the point in which nail crosses the

failure surface($Fpunkt = [nailp(i,5); nailp(i,6)]$). The required angle is obtained as fallow:

$$alphanail(i,1) = pi/2 - atan2(p6(2) - nailp(i,6), p6(1) - nailp(i,5))$$

3.4 Calculating tensile force

Programming process flow chart

1. Determining u_E

2. Determining passive length L

3. First Assumption:

$u_{t1} = 0{,}5.u_E$

$T(L)$

Else

$u_{t2} \neq u_{t1}$

$(\frac{u_{t2} - u_{t1}}{u_{t1}} \approx 2\%)$

if

$u_{t2} = u_E - \Delta L_{p1}$

$\Delta L_{p1} = \frac{0{,}7.T(L)}{EA} \cdot Lp$

Lp= nail length behind the failure surface

$T(L)$

Else

$u_{t2} \neq u_{t1}$

if

$u_{t2} = u_E - \Delta L_{p1}$

$\Delta L_{p1} = \frac{0{,}7.T(L)}{EA} \cdot Lp$

Lp= nail length behind the failure surface

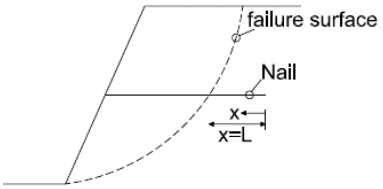

$u_t > u_p$

$u_t \leq u_p$

Numerical method to determine x_p

$f(x_p) = 0$

First assumption $x_p = L/2$

$T(L) = \sqrt{EAD\pi k}\tanh(aL).u_t$

$a = \sqrt{D\pi k/EA}$

x_p = the position in which the peak frictional stress starts to develop

$T(L) = \sqrt{EAD\pi k}\tanh(ax_p).u_p + D\pi\tau_p(L - x_p)$

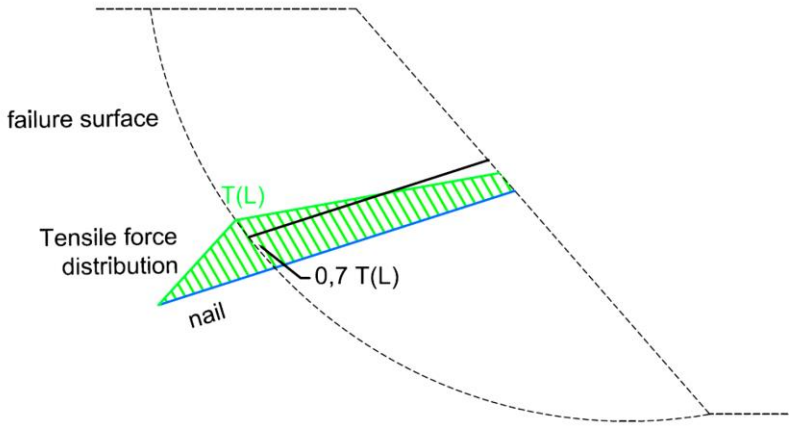

Figure 3.5. Tensile force distribution

To calculate ut, we made three assumptions:

1. The distribution of tensile force along the nail is as shown in figure 3.5 (green part).
2. $u_t = u_E - \Delta L_{p1}$
3. To obtain relative displacement along the part of the nail behind the failure surface ΔL_{p1} we assumed that tensile force distribution is constant and is a percentage of tensile force at the failure surface $0.7T(L)$(black part). This percent is considered as a parameter which can be changed.

$$\Delta L_{p1} = \frac{0{,}7.T(L)}{EA} \cdot (L - Lp)$$

Tensile Force

$K =$ Nail stiffness $= tp/up$

$a = sqrt(Dc * pi * K/(Es * A))$

int is defined to specify the number of rotation angles. Its interval can be changed

$$0.1 \leq int \leq o.6 \quad int(i+1) - int(i) = 0.1$$

$results1$ is a matrix that will store the amounts of rotation angles $tetta$ and their related relative displacements ut and us of each nail

$$results1 = [tetta, ut1(cm), ut2(cm), \dots, utn(cm), us1(cm), us2(cm), \dots, usn(cm)]$$

$results2$ will store passive length of nails Lp and displacements uE regarding to rotation angles $tetta$

$$results2 = [tetta\ Lp1(m)\ Lp2(m) \dots Lpn(m)\ uE1(cm)\ uE2(cm) \dots uEn(cm)]$$

$results3$ will store the amounts of rotation angles $tetta$ and their related

1- tensile and shear forces Ft and Fsh mobilized in nails and
2- factor of safeties using Bishop method and Spencer method
3- obtained Lambda value that made the two factor of safeties equal using Spencer method

$$results3 = [tetta, Ft1(kN), Ft2(kN), \dots, Ftn(kN), Fsh1(kN), Fsh2(kN), \dots, Fshn(kN), FOSb, FOSsp, Lambda]$$

$int2$ will be used to calculate factor of safety with respect to different $lambda$ values

$$0 \le int2 \le num \quad int2(i+1) - int2(i) = 0.2$$

$$results1 = zeros(length(int), 2 * nnail + 1)$$

$$results2 = zeros(length(int), 2 * nnail + 1)$$

$$results3 = zeros(length(int), 2 * nnail + 4)$$

$$ii = 0$$

$xptetta$ will store the amounts of relative displacement xp regarding to rotation angles when $ut < up$

$$xptetta = zeros(length(int), nnail + 1)$$

$$Ftmax = zeros(3,2)$$

for $0.1 \le tetta \le o.6 \quad tetta(i+1) - tetta(i) = 0.1$

$$ii = ii + 1$$

$$xptetta(ii, 1) = tetta$$

$tetta = tetta * pi/180$ ($tetta$ in radian)

for $n = 1{:}\, nnail$

$$Ftmax(n, 1) = n$$

Calculating part of the nail length which is pulled out from the soil surface (parameters are shown in figure 3.6).

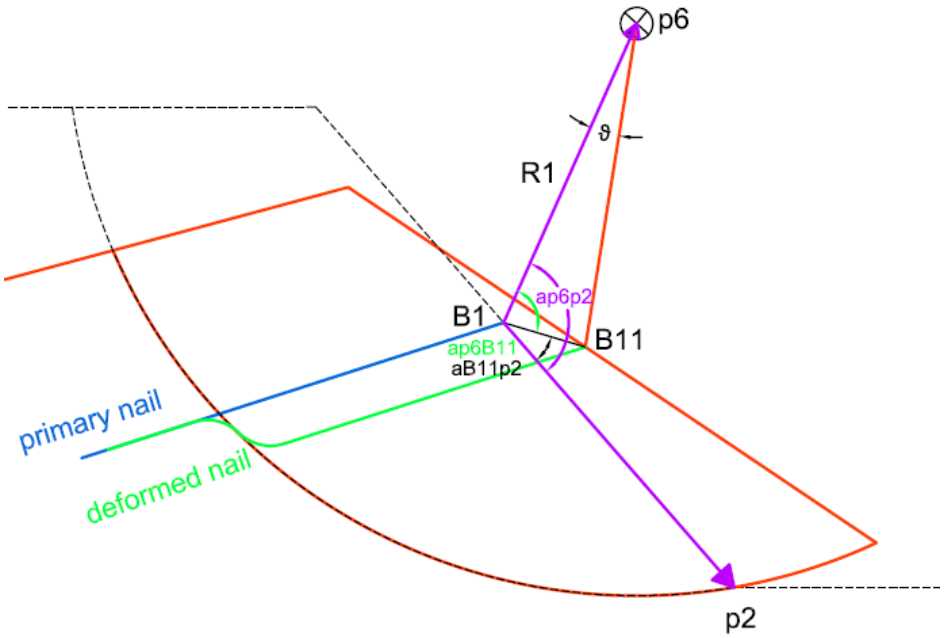

Figure 3.6. Parameters to calculate uE

$B1 = [nailp(n,1); nailp(n,2)]$

$R1 = norm(B1 - p6)$ (Distance of nail head B1 from center point p6)

$B1p6 = p6 - B1$ (A vector from B1 to p6)

$B1p2 = p2 - B1$ (A vector from B1 to p2)

$ap6p2 = acos(dot(B1p6, B1p2)/(norm(B1p6) * norm(B1p2)))$ (Angle between $B1p6$ and $B1p2$ in radian)

$ap6B11 = (pi - tetta)/2$ (Angle)

$aB11p2 = ap6p2 - ap6B11$ (Angle)

$LB1B11 = sin(tetta) * R1/sin(ap6B11)$ (Length between B1 & B11)

$uE = sin(aB11p2) * LB1B11/sin(pi - (betta + a1))$ (Pull out length)

$aB1B11 = betta + a1 - aB11p2$ (Angle)

$us = LB1B11 * sin(aB1B11)$ (Relative displacement normal to nail length)

$ut2 = 0$

First assumption for ut :

$ut = 0.5 * uE$

utt refers to the accuracy of determined ut

$utt = abs(ut2 - ut)/ut$

$Lp = nails(n, 2)$ (Passive length)

$count\_max = 10$ is defined to check if a special $tetta$ makes the loop operates infinitely)

$count = 0$

while $(utt > 0.02)$ && $(count < count\_max)$

$count < count\_max$ is considered to prevent of loop operating infinitely

$count = count + 1$

if $ut \leq up$ it means that if the magnitude of the mobilized displacement at the failure surface is less than the magnitude of displacement causing peak shear stress at the interface of soil and nail

$Ft = (sqrt(Es * A * Dc * pi * K)) * tanh(a * Lp) * ut$

$Ft =$ Tensile force developed in the nail at failure surface

$percent = 0.7$

$dLp1 = percent * Ft * (L1 - Lp)/(Es * A)$

$ut2 = uE - dLp1$

$utt = abs(ut2 - ut)/ut$

$ut = ut2$ (Displacement at failure surface $x = Lp$)

$utxp = ut$

else

break (it means to leave the loop while)

end

end

if $ut <= up$ (calculating xp when $ut < up$)

$g1 = @(x11)\ tp - K * utxp * cosh(a * x11)/cosh(a * Lp)$

$xpg1 = fzero(g1, L1)$

$xptetta(ii, n + 1) = xpg1$

end

for the state $ut > up$ we should define again some assumptions such as:

$ut2 = 0$

$utt = abs(ut2 - ut)/ut$

$count\_max = 10$ is defined to check if a special $tetta$ makes the loop operates infinitely)

$count = 0$

while $(utt > 0.02)$ && $(count < count\_max)$

$count = count + 1$

if $ii > 2$ it means that the number of $tetta$ (rotation angle) should be more than 2 to calculating following equations

if $ut > up$

$xptetta(ii, n+1) = xptetta(ii-1, n+1) + (xptetta(ii-2, n+1) - xptetta(ii-1, n+1))/(xptetta(ii-2,1) - xptetta(ii-1,1)) * (xptetta(ii,1) - xptetta(ii-1,1))$

if $xptetta(ii, n+1) > 0$

$Ft = sqrt(Es * A * Dc * pi * K) * tanh(a * xptetta(ii, n+1)) * up + Dc * pi * tp * (Lp - xptetta(ii, n+1))$

$Ft =$ Tensile force developed in the nail at failure surface

$percent = 0.7$

$dLp1 = percent * Ft * (L1 - Lp)/(Es * A)$

$ut2 = uE - dLp1$

$utt = abs(ut2 - ut)/ut$

$ut = ut2$ (Displacement at failure surface $x = Lp$)

$Ftmax(n, 2) = Ft$

else

$Ft = Ftmax(n, 2)$

break

end

else

$Ft = (sqrt(Es * A * Dc * pi * K)) * tanh(a * Lp) * ut$

$percent = 0.7$

$dLp1 = percent * Ft * (L1 - Lp)/(Es * A)$

$ut2 = uE - dLp1$

$utt = abs(ut2 - ut)/ut$

$ut = ut2$

end

else

In this state it will be displayed that the number of rotation angles is not sufficient to calculate tensile force

disp('$nail$')

disp(n)

disp('$tetta$')

disp($tetta * 180/pi$)

disp(' $ii \leq 2$ ')

break

end

end

Shear force

Calculating the shear force using Eq. (17) discussed in the previous chapter (2.4.3) gives values greater than maximum allowable shear force. Therefore the magnitude of shear force is calculated with respect to the distribution of normal stress along the nail as follow:

$$\begin{cases} \mathrm{Lp} < 1\mathrm{m} & \mathrm{Fsh} = \mathrm{Lp} * 2 * \mathrm{Dc} * \mathrm{Ksh} * \mathrm{us}/2 \\ \mathrm{Lp} \geq 1\mathrm{m} & \mathrm{Fsh} = 1 * 2 * \mathrm{Dc} * \mathrm{Ksh} * \dfrac{\mathrm{us}}{2} \end{cases}$$

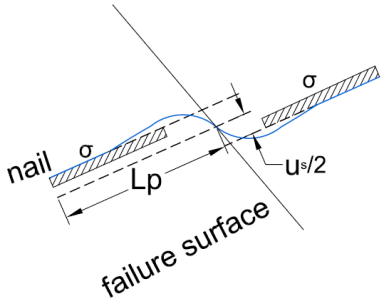

$Fsh = 1m * 2 * Dc * \sigma s$

$\sigma s = Ksh * us/2$

if $count == 10$ (it means that loop operates infinitely at a specified $tetta$)

disp ('<<error in loop for $tetta$ =>>')

disp ($tetta * 180/pi$)

By considering following values, later in the results table we will understand that at which $tetta$ the error had been occurred.

$ut = 0$

$Ft = 0$

$Fsh = 0$

$us = 0$

end

$Ftn = Ft$ (Tensile force)

Matrixes $results1$ and $results2$ and $results3$ include the parameters as follow

$results1 = [tetta, ut1(cm), ut2(cm), \dots, utn(cm), us1(cm), us2(cm), \dots, usn(cm)]$

$results2 = [tetta\ Lp1(m)\ Lp2(m) \dots Lpn(m)\ uE1(cm)\ uE2(cm) \dots uEn(cm)]$

$results3 = [tetta, Ft1(kN), Ft2(kN), \dots, Ftn(kN), Fsh1(kN), Fsh2(kN), \dots,$
$Fshn(kN), FOSb, FOSsp, Lambda]$

$results1(ii, n+1) = ut * 100$

$results1(ii, nnail + n + 1) = us * 100$

$results3(ii, n+1) = Ftn$

$results3(ii, nnail + n + 1) = Fsh$

$results2(ii, n+1) = Lp$

$results2(ii, nnail + n + 1) = uE * 100$

end

3.5 Calculating factor of safety using the Bishop Method

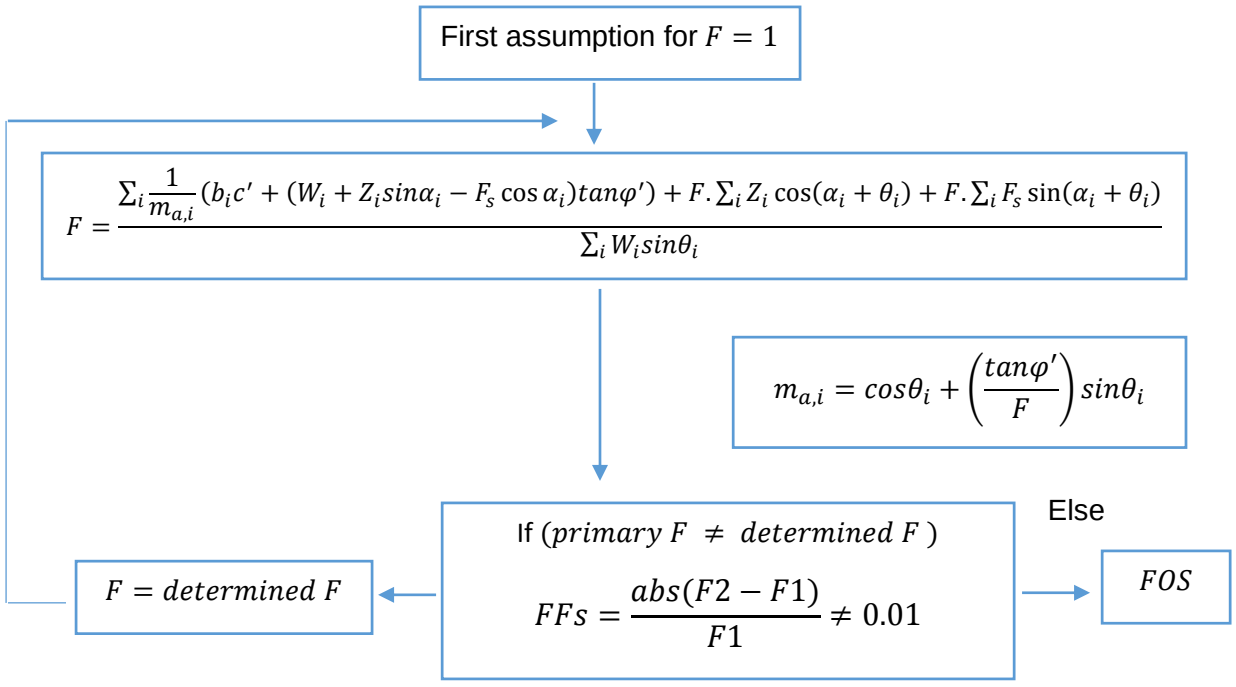

The first assumption for factor of safety

$Fs = 1$

FFs refers to the accuracy of determined Fs, for the beginning we should assume a value for FFs

$FFs = 2$

$Find2 = zeros(nnail, 1)$

$Find3 = zeros(nnail, 1)$

$findf = zeros(ns, 1)$

$wsin = zeros(ns, 1)$

$lcosalpha = zeros(ns, 1)$

for $i = 1{:}\, ns$ (from slide 1 to slide ns)

$wsin(i) = weight(i, 2) * sin(alphaangles(i, 2) * pi/180)$ $(wsin = W * sin(\theta))$

$lcosalpha(i) = L(i, 2) * cos(alphaangles(i, 2) * pi/180)$ $(lcosalpha = l * cos(\theta)$

we will use the Eq. when using Spencer method)

end

while $FFs > 0.01$

$malpha = cos(alphaangles(:,2) * pi/180) + tan(phi)/Fs *$
$sin(alphaangles(:,2) * pi/180)$

$(m_a = \cos\theta + \frac{\tan\phi' \sin\theta}{F})$

for $i = 1{:}\, ns$ (from slide 1 to slide ns)

$findf(i) = (L(i, 2) * cos(alphaangles(i, 2) * pi/180) * cohesion +$
$weight(i, 2) * tan(phi))/malpha(i)$

$(findf = \frac{1}{m_\alpha}(lc' \cos\theta + W \tan\phi'))$

end

for $i = 1{:}\, nnail$ (from nail 1 to slide $nnail$)

$(Find2 = \frac{(T \sin\alpha - F_s \cos\alpha)\tan\phi'}{\cos\theta + \frac{\tan\phi' \sin\theta}{F}})$

$Find2(i) = (results3(ii, i + 1) * sin(a1) - results3(ii, nnail + i + 1) *$
$cos(a1)) * tan(phi)/(cos(alphanail(i)) + tan(phi) * sin(alphanail(i))/Fs)$

$(Find3 = F\ T\ \cos(\alpha + \theta) + F\ F_s \sin(\alpha + \theta))$

$$Find3(i) = Fs * results3(ii, i+1) * cos\big(a1 + alphanail(i)\big) + Fs * results3(ii, nnail + i + 1) * sin(a1 + alphanail(i))$$

end

Factor of safety using Bishop Method

$$F = \frac{\sum \frac{1}{m_a} (lc' \cos\theta + (W + T \sin\alpha - F_s \cos\alpha) \tan\phi' + F \sum T \cos(\alpha + \theta) + F \sum F_s \sin(\alpha + \theta)}{\sum W \sin\theta}$$

$FOSb = (sum(findf) + sum(Find2) + sum(Find3))/(sum(wsin))$

$FFs = abs(FOSb - Fs)/Fs$ (Accuracy)

$Fs = FOSb$

end

$results1 = [tetta, ut1(cm), ut2(cm), \dots, utn(cm), us1(cm), us2(cm), \dots, usn(cm)]$

$results2 = [tetta\ Lp1(m)\ Lp2(m) \dots Lpn(m)\ uE1(cm)\ uE2(cm) \dots uEn(cm)]$

$results3 = [tetta, Ft1(kN), Ft2(kN), \dots, Ftn(kN), Fsh1(kN), Fsh2(kN), \dots, Fshn(kN), FOSb, FOSsp, Lambda]$

$results1(ii, 1) = tetta * 180/pi$

$results2(ii, 1) = tetta * 180/pi$

$results3(ii, 1) = tetta * 180/pi$

$results3(ii, 2 * nnail + 2) = FOSb$ (Bishop Method)

3.6 Calculating Factor of safety using The Spencer Method

$$Sm_i = \frac{l_i}{F}(c' + \sigma_i tan\varphi')$$

$$p_i = \frac{W_i + Z_i sin\alpha_i - \frac{l_i c'}{F}\sin\theta_i - F_s \cos\alpha_i + X_L - X_R}{cos\theta_i + \left(\frac{tan\varphi'}{F}\right) sin\theta_i}$$

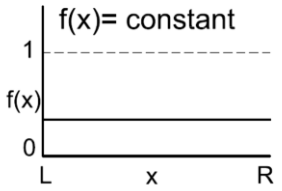

$$X_L = E_L \times \lambda$$
$$X_R = E_R \times \lambda$$

$$0 < \lambda < 0.6$$

specified Fn. —— applied Fn.

$$E_{Ri} = E_{Li} - Sm_i \times \cos(\theta_i) + p_i \times \sin(\theta_i) - Z_i \cos\alpha_i - F_s \sin\alpha_i$$

At first slide (left) $E_L = 0$

$$F_f = \frac{\sum_i (l_i c' + p_i tan\varphi')\cos(\theta_i) + F.\sum_i Z_i \cos(\alpha_i) + F.\sum_i F_{si}\sin(\alpha_i)}{\sum_i p_i sin\theta_i}$$

$$F_m = \frac{\sum_i (l_i c' + p_i tan\varphi') + F.\sum_i Z_i \cos(\alpha_i + \theta_i) + F.\sum_i F_{si}\sin(\alpha_i + \theta_i)}{\sum_i W_i sin\theta_i}$$

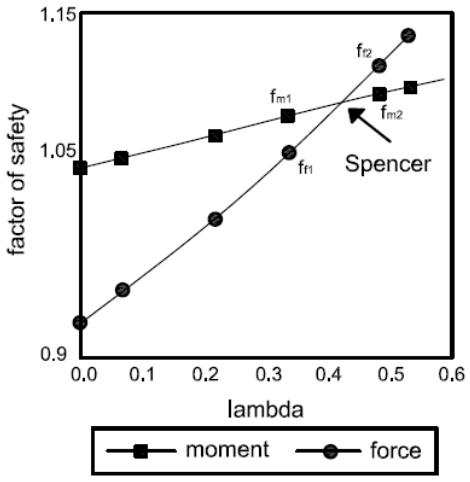

$FOSmatrix = zeros(dnum, 3)$

$im = 0$

$Fa = FOSb$ (First assumption for factor of safety)

$Difh = 1$

$Find4 = zeros(nnail, 1)$

$Find5 = zeros(nnail, 1)$

for $i = 1{:}\, nnail$ (from nail 1 to slide $nnail$)

$(Find4 = T\cos(\alpha + \theta) + F_s \sin(\alpha + \theta))$

$Find4(i) = results3(ii, i+1) * cos(a1 + alphanail(i)) + results3(ii, nnail + i + 1) * sin(a1 + alphanail(i))$

$(Find5 = T\cos\alpha + F_s \sin\alpha)$

$Find5(i) = results3(ii, i+1) * cos(a1) + results3(ii, nnail + i + 1) * sin(a1)$

end

while $Difh > 0.01$

for $lambda = 0{:}\, 0.2{:}\, num$ ($0 \le \lambda \le num$ $\lambda(i+1) - \lambda(i) = 0.2$)

It means that the following statements will be done in the assumed interval of λ

$im = im + 1$

$p = zeros(ns, 1)$ Determined normal forces for all slices will be stored in matrix p

for $i = 1{:}\, ns$ (from slide 1 to slide ns)

$p(i) = weight(i, 2) * cos(alphaangles(i, 2) * pi/180)$ First assumption of normal force

end

$PP = ones(ns, 1)$ The differences between calculated normal forces and previous normal forces will be stored in matrix PP ($PP = Pdetermined - p$)

while $max(abs(PP)) > 0.01$

$$(F = \frac{\sum(lc' + P\tan\phi') + F\sum F_s \sin(\alpha + \theta) + F\sum T\cos(\alpha + \theta)}{\sum W \sin\theta})$$

$F = (sum(L(:,2)) * cohesion + sum(p) * tan(phi) + Fa * sum(Find4))/(sum(wsin))$ (Factor of safety)

$ER = zeros(ns, 1)$ Right horizontal interslice normal forces will be calculated

$EL = zeros(ns, 1)$ left horizontal interslice normal forces will be determined

$mn = nnail$ to calculate right and left interslice normal forces we should know if any resisting forces of nails must be considered in related equations

$EL(ns) = 0$

for $i = 1: ns - 1$ (from slide 1 to slide $ns - 1$)

$(S_m = \frac{l}{F}(c' + \frac{P}{l} tan\varphi'))$

$Sm = L(-i + ns + 1,2)/F * (cohesion + p(-i + ns + 1)/L(-i + ns + 1,2) * tan(phi))$

if $mn > 0$

if $nailp(mn, 5) < Cpoints(1, -i + ns + 1)$

$(E_R = E_L - F_s \sin\alpha - T\cos\alpha + P\sin\theta - S_m\cos\theta = 0)$

$ER(-i + ns + 1) = EL(-i + ns + 1) - Sm * \cos\left(alphaangles(-i + ns + 1,2) * \frac{pi}{180}\right) + p(-i + ns + 1) * sin\left(alphaangles(-i + ns + 1,2) * \frac{pi}{180}\right) - results3(ii, mn + 1) * cos(a1) - results3(ii, nnail + mn + 1) * sin(a1)$

$EL(-i + ns) = ER(-i + ns + 1)$

$mn = mn - 1$

else

$(E_R = E_L + P\sin\theta - S_m\cos\theta = 0$

$ER(-i + ns + 1) = EL(-i + ns + 1) - Sm * cos\left(alphaangles(-i + ns + 1,2) * \frac{pi}{180}\right) + p(-i + ns + 1) * sin(alphaangles(-i + ns + 1,2) * pi/180);$

$EL(-i + ns) = ER(-i + ns + 1)$

end

else

$$ER(-i+ns+1) = EL(-i+ns+1) - Sm * cos\left(alphaangles(-i+ns+1,2) * \frac{pi}{180}\right) + p(-i+ns+1) * sin(alphaangles(-i+ns+1,2) * pi/180);$$

$$EL(-i+ns) = ER(-i+ns+1)$$

end

end

slice 1:

$$(S_m = \frac{l}{F}(c' + \frac{P}{l}tan\varphi'))$$

$$Sm = L(1,2)/F * (cohesion + p(1)/L(1,2) * tan(phi))$$

We assumed that slide 1 doesn't include any nail

$$ER(1) = EL(1) - Sm * cos\left(alphaangles(1,2) * \frac{pi}{180}\right) + p(1) * sin(alphaangles(1,2) * pi/180)$$

$XL = EL * lambda$ Left vertical interslice shear forces

$XR = ER * lambda$ Right vertical interslice shear forces

$Pdetermined = zeros(ns, 1)$ Pdetermined is the determined normal force P

$dd = 1$

for $i = 1{:}ns$ (from slide 1 to slide ns)

if $dd <= nnail$

if $nailp(dd,5) < Cpoints(1, i+1)$

$$(P = \frac{W + T\sin\alpha - \frac{l}{F}c'\sin\theta - F_s\cos\alpha - X_R + X_L}{\cos\theta + \frac{\tan\phi'\sin\theta}{F}})$$

$$Pdetermined(i) = (weight(i,2) - XR(i) + XL(i) - cohesion/F * L(i,2) * sin(alphaangles(i,2) * pi/180) + results3(ii, dd+1) * sin(a1) - results3(ii, nnail+dd+1) * cos(a1))/(cos\left(alphaangles(i,2) * \frac{pi}{180}\right) + \frac{1}{F} * sin(alphaangles(i,2) * pi/180) * tan(phi))$$

$$dd = dd + 1$$

else

$$(P = \frac{W + (\mathrm{X}_L - \mathrm{X}_R) - \frac{c' l \sin\theta}{F}}{\cos\alpha + \frac{\sin\alpha \tan\phi'}{F}})$$

$$Pdetermined(i) = (weight(i,2) - XR(i) + XL(i) - \frac{cohesion}{F} * L(i,2) * sin(alphaangles(i,2) * pi/180))/ (cos\left(alphaangles(i,2) * \frac{pi}{180}\right) + \frac{1}{F} * sin(alphaangles(i,2) * pi/180) * tan(phi))$$

end

else

$$(P = \frac{W + (\mathrm{X}_L - \mathrm{X}_R) - \frac{c' l \sin\theta}{F}}{\cos\alpha + \frac{\sin\alpha \tan\phi'}{F}})$$

$$Pdetermined(i) = (weight(i,2) - XR(i) + XL(i) - \frac{cohesion}{F} * L(i,2) * sin(alphaangles(i,2) * pi/180))/ (cos\left(alphaangles(i,2) * \frac{pi}{180}\right) + \frac{1}{F} * sin(alphaangles(i,2) * pi/180) * tan(phi))$$

end

end

$PP = Pdetermined - p$

$p = Pdetermined$

end

$F1 = F$

$diff1 = 1$ (Accuracy of determined factor of safety)

while $diff1 > 0.01$

$$F_m = \frac{\sum(lc' + P\tan\phi') + F\sum F_s \sin(\alpha + \theta) + F\sum T\cos(\alpha + \theta)}{\sum W \sin\theta}$$

$$Fm = (sum(L(:,2)) * cohesion + sum(p) * tan(phi) + F1 * sum(Find4))/(sum(wsin));$$

$diff1 = abs(Fm - F1)/F1$

$F1 = Fm$

end

$pcosalpha = zeros(ns, 1)$

$psinalpha = zeros(ns, 1)$

for $i = 1{:}\, ns$ (from slide 1 to slide ns)

$(pcosalpha(i) = P * \cos\theta)$

$pcosalpha(i) = p(i) * cos(alphaangles(i, 2) * pi/180)$

$(psinalpha(i) = P * \sin\theta)$

$psinalpha(i) = p(i) * sin(alphaangles(i, 2) * pi/180)$

end

$diff2 = 1$

$F2 = F$

while $diff2 > 0.01$

$$F_f = \frac{\sum(lc' + P\tan\phi')\cos\theta + F\sum(F_s\sin\alpha + T\cos\alpha)}{\sum P\sin\theta}$$

$Ff = (sum(lcosalpha) * cohesion + sum(pcosalpha) * tan(phi) + F2 * sum(Find5))/(sum(psinalpha))$

$diff2 = abs(Ff - F2)/F2$

$F2 = Ff$

end

Where the curves of Fm and Ff cross each other is the Spencer factor of safety

$FOSmatrix(im, 1) = lambda$

$FOSmatrix(im, 2) = Fm$

$FOSmatrix(im, 3) = Ff$

end

Following statements are written to draw a diagram that shows how the moment and force factors of safety vary with lambda

for $iii = 1{:}\,(dnum - 1)$

if $(FOSmatrix(iii, 2) - FOSmatrix(iii, 3)) * (FOSmatrix(iii + 1{,}2) - FOSmatrix(iii + 1{,}3)) < 0$ $\quad((Fm(i) - Ff(i)) * (Fm(i+) - Ff(i + 1)) < 0)$

$aa1 = (FOSmatrix(iii + 1,3) - FOSmatrix(iii, 3))/(FOSmatrix(iii +$

$1,1) - FOSmatrix(iii, 1))$ $(aa1 = \frac{Ff(i+1)-Ff(i)}{\lambda(i+1)-\lambda(i)})$

Equation of line Ff:

$bb1 = FOSmatrix(iii, 3) - aa1 * FOSmatrix(iii, 1)$

$aa2 = (FOSmatrix(iii + 1,2) - FOSmatrix(iii, 2))/(FOSmatrix(iii +$

$1,1) - FOSmatrix(iii, 1))$ $(aa2 = \frac{Fm(i+1)-Fm(i)}{\lambda(i+1)-\lambda(i)})$

Equation of line Fm:

$bb2 = FOSmatrix(iii, 2) - aa2 * FOSmatrix(iii, 1)$

$xlambda = (bb2 - bb1)/(aa1 - aa2)$

$ylambda = aa1 * xlambda + bb1$

$Factorofsafety = ylambda$

$determinedLAMBDA = xlambda$

break

end

end

$Difh = abs(Factorofsafety - Fa)/Fa$

$Fa = Factorofsafety$

end

$results3(ii, 2 * nnail + 3) = Factorofsafety$ (Obtained Spencer factor of safety)

$results3(ii, 2 * nnail + 4) = determinedLAMBDA$

end

end

3.7 Displaying results

disp('$results1 = [tetta\ ut(cm)\ us(cm)]$')

disp(results1)

disp('$results2 = [tetta\ Lp(m)\ uE(cm)]$')

disp(results2)

disp('$xptetta = [tetta\ xp]$')
disp(xptetta)

disp('$results3 = [tetta\ Ft(kN)\ Fsh(kN)\ FOSb\ FOSsp\ Lambda]$')
disp(results3)

Figure of slope

Line $([p1(1), p2(1)], [p1(2), p2(2)], 'Color', [.7\ .5\ 0], 'LineWidth', 1.5)$
Line $([p2(1), p3(1)], [p2(2), p3(2)], 'Color', [.7\ .5\ 0], 'LineWidth', 1.5)$
Line $([p3(1), p4(1)], [p3(2), p4(2)], 'Color', [.7\ .5\ 0], 'LineWidth', 1.5)$

Displaying center point

Plot $(p6(1), p6(2), 'Marker', 'p', 'Color', [.1\ .3\ 0.5], 'MarkerSize', 5)$

Drawing of nails

for i=1:nnail
- $B1 = [nailp(i, 1); nailp(i, 2)]$
- $B2 = [nailp(i, 3); nailp(i, 4)]$
- line($[B1(1), B2(1)], [B1(2), B2(2)], 'Color', [1\ .5\ 0], 'LineWidth', 1.5$)

end

for $i = 1{:}\ nnail$ (for nail 1 to nail nnail)
- plot($xptetta(:, 1), xptetta(:, i + 1), 'r*'$)
- xlabel('$tetta(0.04{:}\ 0.03{:}\ 0.65)$')
- ylabel('$xp(meter)$')

end

3.8 Example

The design parameters used for this example were as follows; height of slope $= 6m$, slope angle $= 75°$, number of nails $= 4$, nail length $= 4\,m$, inclination angle of nail $= 10°$, unit weight of soil $= 21\,kN/m3$, $c = 0$, $\phi = 30\,°$, elastic modulus of the steel nail $= 21e7\,kN/m^2$, diameter of nail hole $= 0.076\,m$, diameter of steel rod (nail) $= 0.038\,m$, vertical distance of the nails heads from the ground $= 2\,m, 3\,m, 4\,m, 5\,m$ (nail number 1 is at the bottom and nail number 4 is at the top of the slope), peak shear stress at the interface of soil and nail $\tau_p = 170\,kN/m\text{^}2$, soil-nail displacement causing peak shear stress $u_p = 0.02\,m$, modulus of lateral soil reaction $K_{sh} = 5000\,kN/m\text{^}3$, and slope rotation angles vary from $0.04°$ to $0.65°$.

The potential failure surface is drawn and the nails are placed in the slope as displayed in figure 3.7. Table 3-1 indicates the measured values of mobilized displacement between soil and nail u_t and u_s regarding to variations of slope rotation angles ϑ. The calculated tensile and shear forces mobilized in the nails and the related Bishop factor of safety are listed in table 3-2.

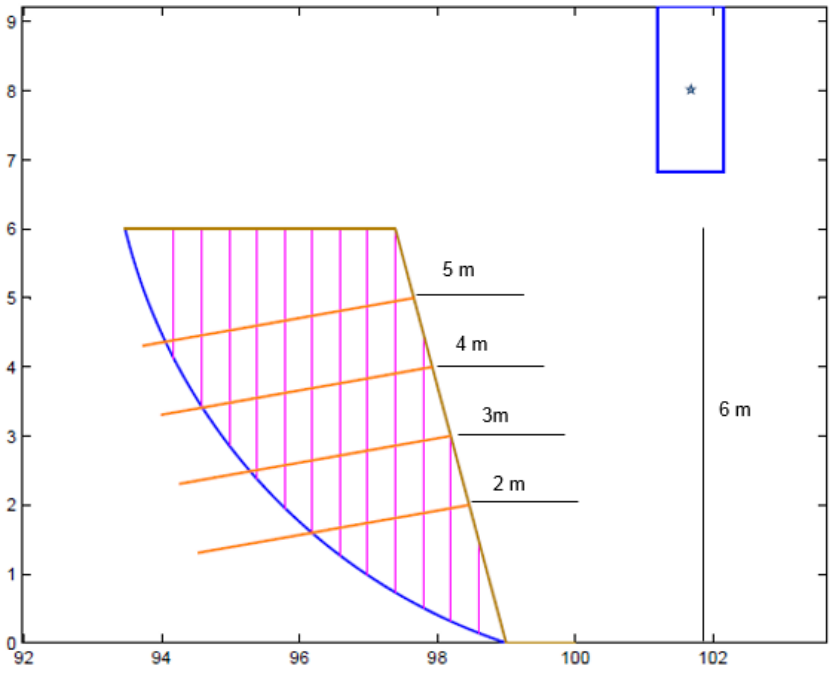

Figure 3.7. Schematic of soil nailed slope

Table 3-1

$tetta(°)$	$ut1(cm)$	$ut2(cm)$	$ut3(cm)$	$ut4(cm)$	$us1(cm)$	$us2(cm)$	$us3(cm)$	$us4(cm)$
0.04	0.34128	0.27165	0.20163	0.13061	0.29411	0.30043	0.30676	0.31308
0.07	0.59738	0.47554	0.353	0.22872	0.51452	0.52562	0.53672	0.54782
0.1	0.85384	0.67967	0.50454	0.32696	0.73478	0.75068	0.76659	0.7825
0.13	1.1103	0.88384	0.65618	0.42533	0.95489	0.97563	0.99637	1.0171
0.16	1.3668	1.0881	0.80794	0.52382	1.1749	1.2005	1.2261	1.2517
0.19	1.6235	1.2926	0.95983	0.62244	1.3947	1.4252	1.4557	1.4861
0.22	1.8803	1.4971	1.1119	0.72119	1.6144	1.6498	1.6852	1.7206
0.25	2.1401	1.7018	1.264	0.82006	1.8339	1.8742	1.9146	1.9549
0.28	2.4212	1.9066	1.4163	0.91907	2.0533	2.0986	2.1439	2.1892
0.31	2.6813	2.1135	1.5687	1.0182	2.2725	2.3228	2.3731	2.4235
0.34	2.9415	2.3375	1.7212	1.1175	2.4916	2.5469	2.6023	2.6576
0.37	3.2018	2.5445	1.8738	1.2168	2.7105	2.7709	2.8313	2.8918
0.4	3.4623	2.7516	2.0277	1.3163	2.9293	2.9948	3.0603	3.1258
0.43	3.7228	2.9589	2.1928	1.416	3.1479	3.2185	3.2892	3.3598
0.46	2.015	3.1663	2.3468	1.5157	3.3664	3.4422	3.5179	3.5937
0.49	2.147	3.3739	2.5009	1.6156	3.5847	3.6657	3.7466	3.8276
0.52	2.279	3.5815	2.6551	1.7157	3.8029	3.8891	3.9752	4.0614
0.55	2.411	3.7893	2.8094	1.8158	4.021	4.1124	4.2037	4.2951
0.58	2.5431	2.0171	2.9639	1.9161	4.2389	4.3355	4.4321	4.5287
0.61	2.6753	2.1221	3.1185	2.0171	4.4566	4.5585	4.6604	4.7623
0.64	2.8076	2.2272	3.2732	2.1248	4.6742	4.7814	4.8887	4.9959

Table 3-2

$tetta(°)$	$Ft1(kN)$	$Ft2(kN)$	$Ft3(kN)$	$Ft4(kN)$	$Fs1(kN)$	$Fs2(kN)$	$Fs3(kN)$	$Fs4(kN)$	FOS
0.04	11.688	5.8011	2.5169	0.90614	1.1176	1.1416	0.71332	0.40533	0.83681
0.07	20.458	10.155	4.4064	1.5868	1.9552	1.9973	1.2481	0.70923	0.90728
0.1	28.9	14.38	6.2588	2.2599	2.7922	2.8526	1.7826	1.013	0.98524
0.13	37.579	18.699	8.1399	2.9398	3.6286	3.7074	2.3169	1.3168	1.0632
0.16	46.262	23.022	10.022	3.6206	4.4645	4.5617	2.851	1.6204	1.1606
0.19	54.95	27.346	11.907	4.3022	5.2998	5.4156	3.3849	1.924	1.2741
0.22	63.642	31.674	13.792	4.9847	6.1345	6.2691	3.9186	2.2275	1.4048
0.25	68.15	36.004	15.68	5.6681	6.9687	7.1221	4.4521	2.5309	1.5073
0.28	68.15	40.337	17.569	6.3524	7.8024	7.9746	4.9854	2.8343	1.5831
0.31	68.15	42.417	19.459	7.0376	8.6354	8.8267	5.5184	3.1375	1.6361
0.34	68.15	42.417	21.351	7.7236	9.4679	9.6783	6.0513	3.4407	1.6725
0.37	68.15	42.417	23.245	8.4105	10.3	10.529	6.5839	3.7438	1.7103
0.4	68.15	42.417	24.071	9.0983	11.131	11.38	7.1163	4.0468	1.7411
0.43	68.15	42.417	24.071	9.787	11.962	12.23	7.6485	4.3497	1.7662
0.46	68.15	42.417	24.071	10.477	12.792	13.08	8.1805	4.6525	1.8031
0.49	68.15	42.417	24.071	11.167	13.622	13.93	8.7123	4.9553	1.8309
0.52	68.15	42.417	24.071	11.858	14.451	14.778	9.2438	5.258	1.8596
0.55	68.15	42.417	24.071	12.55	15.28	15.627	9.7752	5.5606	1.8892
0.58	68.15	42.417	24.071	13.244	16.108	16.475	10.306	5.8631	1.9199
0.61	68.15	42.417	24.071	13.381	16.935	17.322	10.837	6.1655	1.9475
0.64	68.15	42.417	24.071	13.381	17.762	18.17	11.368	6.4679	1.9749

Looking at the table of output 3-1, the mobilized displacements between soil and nails increase by enhancing the rotation angle. Consequently the magnitude of resisting forces developed in the nails increase with increment of mobilized displacements. Results of the calculated factor of safeties depending on rotation angles lead to estimating the rotation(deformation) of the slope that results in $FOS = 1$ (which could be understood as the serviceability state).

4 Conclusion

This thesis proposed a method for calculating tensile and shear forces developed in nails of a soil nailing structure depending on mobilized displacement between soil and nail. Based on the goal of the thesis the following conclusions can be obtained:

- Relative displacements of a nail in any part of the reinforced soil as well as the resisting forces versus mobilized displacement can be predicted by using direct shear test results.
- It should be considered that the rear end of nail moves even if it is microscopically small. The required embedment length is largely affected by material strength of soil and nails and allowable displacements of the nail improved slope itself.
- The amount of tensile force along the nails is calculated depending on the magnitude of relative displacement between soil and nails at the intersection of nails with failure surface. By calculating the soil-nail displacement normal to the direction of nail length, shear force at failure surface is obtained. The relationship between shear forces and relative displacements is affected by the modulus of lateral soil reaction.

An analytical code is developed which can

- calculate soil-nail displacements regarding the variation of soil nail rotation angle by considering some primary assumptions.
- obtain resisting forces developed in the nail at the failure surface using an iterative method.
- Solve the factor of safety for reinforced soil slope using Bishop method.

Results of the calculated factor of safeties depending on rotation angles lead to finding the rotation angle that results in $FOS = 1$ (limit equilibrium). Regarding the maximum material strength of the nails and the soil resisting forces cannot exceed a certain value and consequently the maximum factor of safety can be achieved. Based on the present model a certain deformation (rotation) of the slope is shown for this maximum factor of safety.

As Bishop Method includes interslice normal forces and ignores the interslice shear forces. In addition I started to analyze slope stability using Spencer method that includes

all interslice forces and satisfy all equations of statics. Developing codes to solve Spencer factor of safety need further works which should be done in a next master thesis.

References

Abramento, Mauricio, and Andrew J. Whittle. "Analysis of Pullout Tests for Planar Reinforcements in Soil." Journal of Geotechnical Engineering J. Geotech. Engrg. 121.6 (1995): 476-85.

Bishop, A. W., and Norbert Morgenstern. "Stability coefficients for earth slopes." Geotechnique 10.4 (1960): 129-153.

Bishop, A. W., et al. "A new ring shear apparatus and its application to the measurement of residual strength." Geotechnique 21.4 (1971): 273-328.

Bridle, R. J. "Soil nailing-analysis and design: Ground Engng V22, N6, Sept 1989, P52–56." International Journal of Rock Mechanics and Mining Sciences & Geomechanics Abstracts. Vol. 27. No. 2. Pergamon, 1990.

Bridle, R. J., and M. C. R. Davies. “Analysis of soil nailing using tension and shear: Experimental observations and assessment.” Proceedings of the ICE-Geotechnical Engineering 125.3 (1997): 155-167.

Bromhead, E. N. "The Stability of Slopes Blackie Academic and Professional."G, B (1992).

Byrne, R. John. "Soil nailing: a simplified kinematic analysis." Grouting, Soil Improvement and Geosynthetics. ASCE, 1992.

Delmas, P. “Mobilisation des efforts dans les ouvrages cloues. Etude comparative de differentes methods de calcul.” Bull liason lab ponts chauss 147(1987).

Fellenius, Wolmar. "Calculation of the stability of earth dams." Transactions of the 2nd congress on large dams, Washington, DC. Vol. 4. International Commission on Large Dams (ICOLD) Paris, 1936.

Gassler, Günter. Vernagelte Geländesprünge--Tragverhalten und Standsicherheit. No. 108. Institut für Bodenmechanik und Felsmechanik der Univerrsität Fridericiana in Karlsruhe, 1987.

GEO. 2008. Geoguide 7 — Guide to soil nail design and construction. Geotechnical Engineering Office (GEO), Civil Engineering and Development Department, The Government of the Hong Kong Special Administrative Region. GEO report No. 197. ISBN: 978-962-02-0375-6.

Guo, Wei Dong. "Pile capacity in nonhomogeneous softening soil." 地盤工学会論文報告集 41.2 (2001): 111-120.

Gurung, Netra, and Yushiro Iwao. "Analytical Pull-out Model for Extensible Soil-reinforcements." Doboku Gakkai Ronbunshu 624 (1999): 11-20.

Gurung, Netra. "1-D analytical solution for extensible and inextensible soil/rock reinforcement in pull-out tests." Geotextiles and Geomembranes 19.4 (2001): 195-212.

Hong, Cheng-Yu, Jian-Hua Yin, Wan-Huan Zhou, and Hua-Fu Pei. "Analytical Study on Progressive Pullout Behavior of a Soil Nail." J. Geotech. Geoenviron. Eng. Journal of Geotechnical and Geoenvironmental Engineering 138.4 (2012): 500-07.

Institut fur Bautechnik. Bodenvernagelung system Bauer. Zulassung-Nr. Z20.1-101, Berlin (1986).

Janbu, N. "Application of composite slip surfaces for stability analysis." Proc. European Conf. on Stability of Earth Slopes, Stockholm, 1954. Vol. 3. 1954.

Jewell, R. A., and M. J. Pedley. "Analysis for soil reinforcement with bending stiffness." Journal of geotechnical engineering 118.10 (1992): 1505-1528.

Jewell, R. A., and M. J. Pedley. "Soil nailing design: the role of bending stiffness." Ground Engineering 23.2 (1990).

Juran, I. "Reinforced soil systems-application in retaining structures."Geotechnical Engineering 16.1 (1985).

Juran, Ilan, and Victor Elias. "Soil nailed retaining structures: Analysis of case histories." Soil Improvement@ sA Ten Year Update. ASCE, 1987.

Juran, Ilan, et al. "Kinematical limit analysis for design of soil-nailed structures." Journal of geotechnical engineering 116.1 (1990): 54-72.

Kakurai, M., and J. Hori. "Soil-reinforcement with steel bars on a cut slope."Performance of Reinforced Soil Structures, Proceedings of the International Reinforced Soil Conference, British Geotechnical Society. 1990.

Kim, J. S., J. Y. Kim, and S. R. Lee. "Analysis of soil nailed earth slope by discrete element method." Computers and Geotechnics 20.1 (1997): 1-14.

Krahn, John. "Stability modeling with Slope/W." Geo-Slope/W International LTD(2012).

Leshchinsky, Dov. "Discussion of “Kinematical Limit Analysis for Design of Soil-Nailed Structures” by Ilan Juran, George Baudrand, Khalid Farrag, and Victor Elias,(January, 1990, Vol. 116, No. 1)." Journal of Geotechnical Engineering 117.11 (1991): 1821-1824.

Madhav, M.r., N. Gurung, and Y. Iwao. "A Theoretical Model for the Pull-Out Response of Geosynthetic Reinforcement." Geosynthetics International 5.4 (1998): 399-424. Web.

Manual of Soil Laboratory Testing. Permeability, Shear Strength and Compressibility Tests; John Wiley & Sons, Inc., New York, 1994.

Misra, Anil, and C-H. Chen. "Analytical solution for micropile design under tension and compression." Geotechnical & Geological Engineering 22.2 (2004): 199-225.

Misra, Anil, et al. "Simplified analysis method for micropile pullout behavior."Journal of geotechnical and geoenvironmental engineering 130.10 (2004): 1024-1033.

Mitachi, T., Y. Yamamoto, and S. Muraki. "Estimation of in-soil deformation behavior of geogrid under pull-out loading." Proceedings of the International Symposium on Earth Reinforcement Practice, Japan. Vol. 1. 1992.

Mitchell, James K., Willem C. B. Villet, and Jerold A. Bishop. Reinforcement of Earth Slopes and Embankments. Washington, D.C.: Transportation Research Board, National Research Council, 1987. Print.

Morgenstern, N. R., and J. S. Tchalenko. "Microscopic structures in kaolin subjected to direct shear." Geotechnique 17.4 (1967): 309-328.

Morgenstern, N. R., and V. Eo Price. "The analysis of the stability of general slip surfaces." Geotechnique 15.1 (1965): 79-93.

Osano, S. N. "Direct shear box and ring shear test comparison: why does internal angle of friction vary." ICASTOR Journal of Engineering 5.2 (2009): 77-93.

Pedley, Martin John. The performance of soil reinforcement in bending and shear. Diss. University of Oxford, 1990.

Petterson, Knut E. "The early history of circular sliding surfaces."Geotechnique 5.4 (1955): 275-296.

Plumelle, C., and F. Schlosser. "A French National Research Project on soil Nailing: Clouterre. Performance of Reinforced Soil Structure." (1990): 0-0.

Schlosser, F. "Analogies et différences dans le comportement et le calcul des ouvrages de soutènement en Terre Armée et par clouage du sol." ANN ITBTP418 (SOLS FOND184) (1983).

Schlosser, F. "Behaviour and design of soil nailing." Proceeding on Recent Developments in Ground Improvement Techniques, Bangkok, Thailand (1982): 29-30.

Schlosser, F., P. Unterreiner, and C. Plumelle. "French research program CLOUTERRE on soil nailing." Grouting, Soil Improvement and Geosynthetics. ASCE, 1992.

Shen, C. K., et al. "An in situ Earth reinforcement lateral support system."NASA STI/Recon Technical Report N 82 (1981): 26520.

Spencer, E. "A method of analysis of the stability of embankments assuming parallel inter-slice forces." Geotechnique 17.1 (1967): 11-26.

Stocker, Manfred F., and Georg Riedinger. "The bearing behaviour of nailed retaining structures." Design and Performance of Earth Retaining Structures. ASCE, 1990.

Wang, Zhenggui, and Werner Richwien. "A Study of Soil-Reinforcement Interface Friction." J. Geotech. Geoenviron. Eng. Journal of Geotechnical and Geoenvironmental Engineering 128.1 (2002): 92-94.

Zhou, Wan-Huan, and Jian-Hua Yin. "A Simple Mathematical Model for Soil Nail and Soil Interaction Analysis." Computers and Geotechnics 35.3 (2008): 479-88.

Zhou, Wanhuan. Experimental and theoretical study on pullout resistance of grouted soil nails. Diss. The Hong Kong Polytechnic University, 2008.